

**Reassessment of N₂ Activation by Low-Valent Ti-Amide Complexes:
A Remarkable Side-On Bridged bis-N₂ Adduct is Actually an Arene Adduct**

Daniel N. Huh^a, Ross F. Koby^a, Zoe E. Stuart^a, Rachel J. Dunscomb^a,
Nathan D. Schley^{*b}, Ian A. Tonks^{*a}

^aDepartment of Chemistry, University of Minnesota – Twin Cities, Minneapolis,
MN 55455, United States.

^bDepartment of Chemistry, Vanderbilt University, Nashville,
TN 37235, United States

Supplementary Information

TABLE OF CONTENT

NMR DATA

Figure S1. Evans' Method of a PhMe solution of 6-K with PhMe capillary.	S4
Figure S2. 400 MHz, C ₆ D ₆ , 25 °C, ¹ H NMR spectrum of 6-K and addition of 10% HCl/H ₂ O solution.	S4

Figure S3. 400 MHz, C ₆ D ₆ , 25 °C, ¹ H NMR spectrum of 9 .	S5
Figure S4. 400 MHz C ₆ D ₆ , 25 °C, ¹ H NMR spectrum of 10 .	S5

X-RAY CRYSTALLOGRAPHIC DATA

Figure S5. Electron density contour map of 5-Li modeled.	S7
--	----

Figure S6. Electron density contour map of 5-Li modeled as 6-Li .	S8
--	----

Table S1. Crystal data and structure refinement for 6-K .	S9
---	----

Table S2. Selected bond lengths [Å] and angles [°] for 6-K .	S10
--	-----

Table S3. Crystal data and structure refinement for the newly collected 6-Li .	S13
--	-----

Table S4. Selected bond lengths [Å] and angles [°] for the newly collected 6-Li .	S14
---	-----

Table S5. Crystal data and structure refinement for 7 .	S15
---	-----

Table S6. Selected bond lengths [Å] and angles [°] for 7 .	S16
--	-----

Table S7. Crystal data and structure refinement for 8 .	S17
---	-----

Table S8. Selected bond lengths [Å] and angles [°] for 8 .	S18
--	-----

Table S9. Selected bond lengths [Å] and angles [°] for 8·THF .	S19
--	-----

Table S10. Selected bond lengths [Å] and angles [°] for 8·THF .	S20
---	-----

Table S11. Crystal data and structure refinement for 9 .	S21
--	-----

Table S12. Selected bond lengths [Å] and angles [°] for 9 .	S22
Table S13. Crystal data and structure refinement for 10 .	S24
Table S14. Selected bond lengths [Å] and angles [°] for 10 .	S25
Table S15. Selected bond distance ranges (Å) and angles (°) of the Ti-arene moieties.	S26
CALCULATIONS	
Computational Methods and Investigations	S26
Figure S6. Summary of DFT analyses of 6-Li , 6-K , and 5⁻ .	S27
Frontier Orbitals of 6-Li	
Figure S7. Summary of DFT analyses of 6-Li , 6-K , and 5⁻ .	S28
Figure S8. SOMO β (unoccupied) centered on ligands of Li ⁺ .	S29
Figure S9. SOMO α (occupied) showing delta bonding between one Ti atom and arene, and sigma bonding between other Ti atom and arene.	S29
Figure S10. HOMO showing delta bonding between both Ti atoms and arene.	S30
Figure S11. HOMO-1 showing delta bonding between both Ti atoms and arene.	S30
Frontier Orbitals of 6-K	
Figure S12. LUMO centered on arene interaction with K ⁺ .	S31
Figure S13. SOMO β (unoccupied) centered on the arene interaction with K ⁺ .	S31
Figure S14. SOMO α (occupied) showing delta bonding between one Ti atom and arene, and sigma bonding between other Ti atom and arene.	S32
Figure S15. HOMO showing delta bonding between both Ti atoms and arene.	S32
Figure S16. HOMO-1 showing delta bonding between both Ti atoms and arene.	S33
Attempted Optimizations of 5⁻	
Figure S17. The calculated structure of 5⁻ as a quartet from crystallographic coordinates optimizes to yield a coordinated end-on dinitrogen and $\mu_2\text{-}\eta^2\text{:}\eta^1$ coordinated dinitrogen.	S33
Figure S18. The calculated structure of 5⁻ as a doublet from crystallographic coordinates optimizes to yield a dissociated dinitrogen (3.12 Å to closest Ti) and bridging nitrides.	S34

Figure S19. LUMO of 10 depicting N–N pi bonding and Ti–N pi anti-bonding.	S35
Figure S20. HOMO of 10 depicting Ti–N pi bonding.	S35
Figure S21. HOMO-1 of 10 depicting Ti–N pi bonding (orthogonal to HOMO).	S36
Figure S22. HOMO-33 of 10 depicting continuous Ti–N–N–Ti pi bonding.	S37
UV-VIS DATA	
Figure S23. UV-vis spectrum of 6-K in toluene.	S38
Figure S24. UV-vis spectrum of 6-Li in 10:1 toluene:TMEDA.	S38
Figure S25. UV-vis spectrum of 10 in pentane.	S39
RAMAN DATA	
Figure S26. Raman of 6-K in toluene using a 457 nm laser.	S39
Figure S27. Raman of 6-Li in 10:1 toluene:TMEDA using a 457 nm laser.	S40
Table S16. Comparison of select bond N–N bond distances and Raman N–N stretch frequencies.	S41
Routing Keywords and Energies	S41
REFERENCES	S43

NMR Data

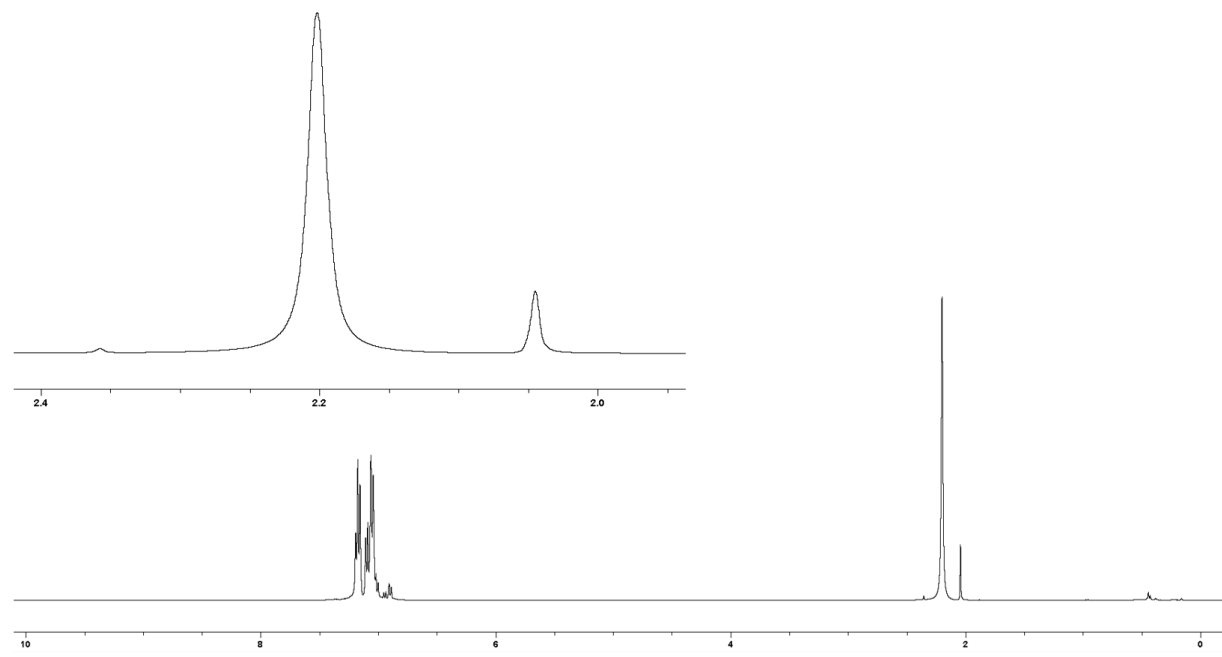


Figure S1. 400 MHz ¹H NMR spectrum Evans' Method of a 20 mM PhMe solution of **6-K** with PhMe capillary.

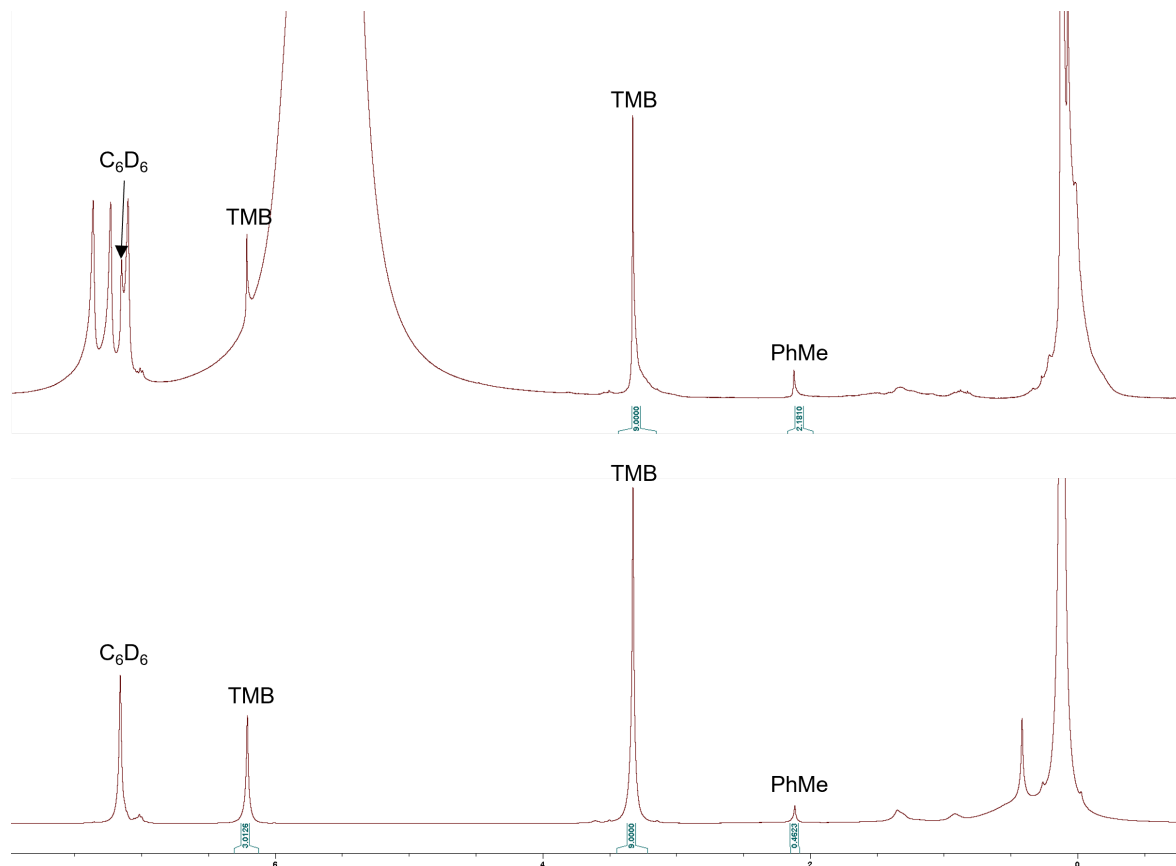


Figure S2. 400 MHz ¹H NMR spectrum in C_6D_6 sample of **6-K** with TMB standard (bottom) and 0.5 mL of 10% HCl solution in H_2O added to the **6-K** sample (top).

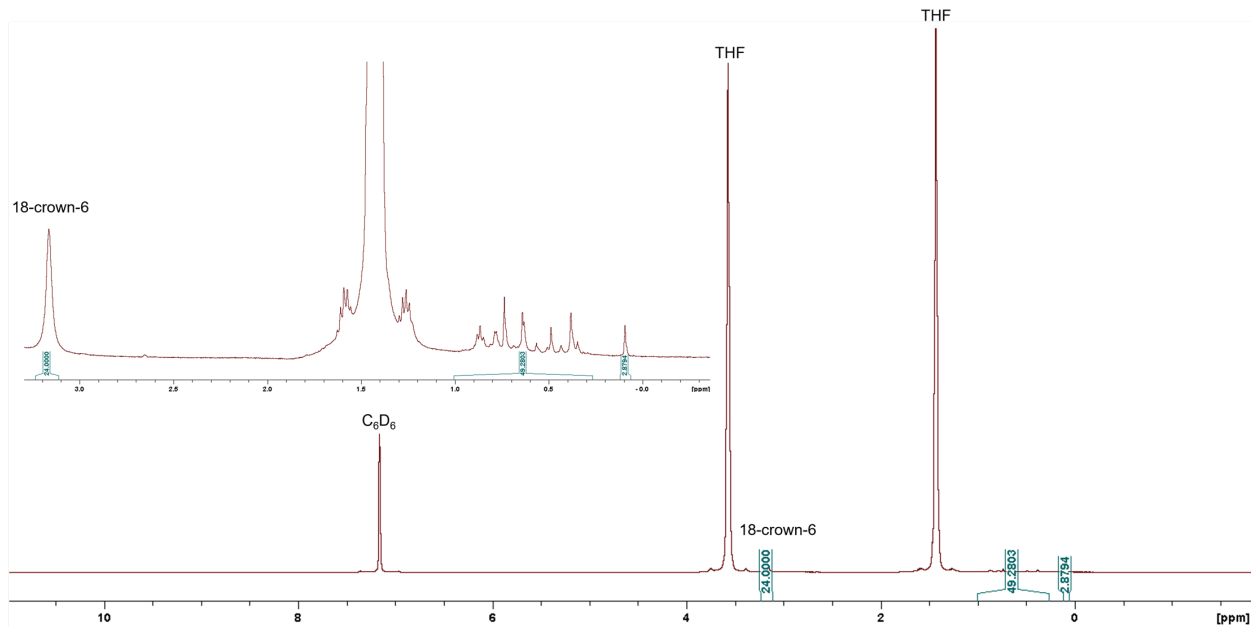


Figure S3. 400 MHz C₆D₆, 25 °C, ¹H NMR spectrum of **9** and expanded region (inset).

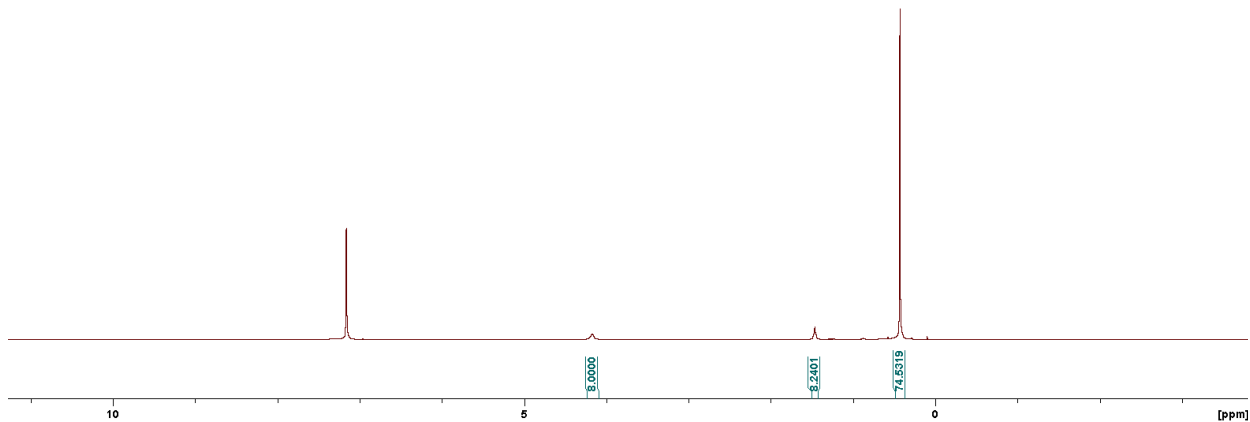


Figure S4. 400 MHz ¹H NMR spectrum of **10**, C₆D₆.

X-ray Crystallographic Data

Details of crystallographic refinement

Treatment of previously reported X-ray structure of 5-Li (JOHBEN, deposition number 1188315). While the atomic coordinates of **5-Li** could be easily retrieved from the Cambridge crystallographic database under deposition number 1188315, the reflection intensities were unavailable from the database. This was not surprising, since routine deposition of structure factors did not become common until the last decade. Fortunately, the structure factors for **5-Li** had been published in printed form as supporting information, and were available to download in pdf format. The software package Tabula¹ was employed to extract tabulated structure factors (reported as 10Fo and 100σFo) which were transformed into hklf3 format using Microsoft Excel.

Modeling 5-Li as a disordered pair of bound N₂ molecules. Refinement of the published coordinates against the extracted structure factors required selection of a suitable occupancy refinement model for the nitrogen positions since these were unavailable in the published work. We applied a model where the sum of the occupancy over the 6 sites was equal to 4. Modeling two fully-occupied dinitrogen molecules over 6 atom positions requires an average occupancy of 2/3 per site, however owing to symmetry, N4 represents 4 of those positions and N3 represents 2. The occupancy was therefore refined using a linear combination such that the 4*Occ(N4) + 2* Occ(N3) = 4. Final refined occupancies were 0.718(13) and 0.641(7) for N3 and N4 respectively. A disordered trimethylsilyl group was also modeled using similarity restraints placed on the atomic thermal parameters and Si-C bond lengths. This model gave near-identical metrics to those published, as would be expected. A map of unmodeled density revealed a peak equal to 0.64 e⁻/Å³ at a distance of 1.57 Å away from one of the nitrogen atom sites (N4). A contour map of Fo showing the arrangement of the nitrogen sites as well as the four positions with positive electron density nearby is given in Figure S5.

Plane: 0.6338x-22.2843y 0.9207z = -0.8864 Cont-Lev(eA-3): -0.60 3.80 0.20 Fo-Map
 Tol = 1.5 Ång Step = 0.0000 Ång Resolution 18.7 Deg. Omtt 2*SlgI

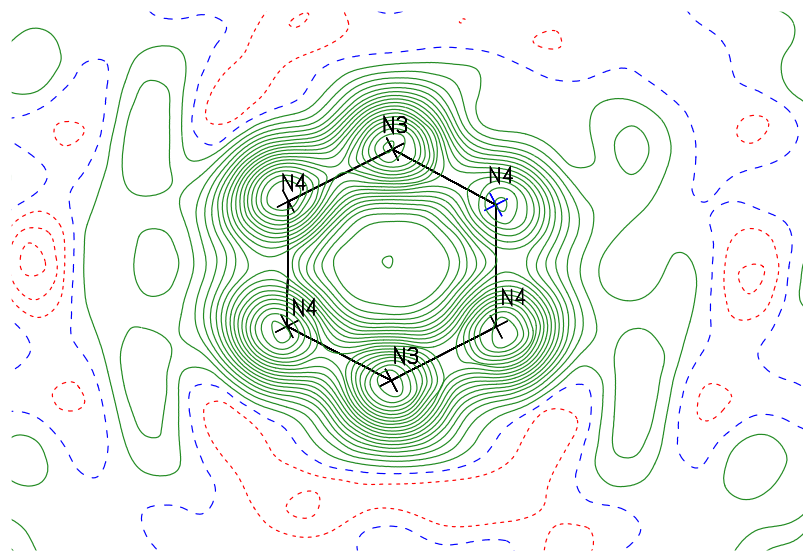


Figure S5. Electron density contour map of **5-Li** modeled as two disordered N_2 molecules. $R_1 = 0.063$, $wR_2 = 0.179$.

*Modeling **5-Li** as a disordered toluene.* Remodeling the disordered pair of N_2 molecules as a full-occupied toluene molecule disordered over four symmetry-related orientations gave an improved R-factor and a smaller largest unmodeled peak in the difference map. In this model, the $\frac{1}{4}$ -occupied methyl site coincides with the largest electron peak in the previous N_2 model. The magnitude of the improvement in R-factor is relatively small owing to the low quality of the original diffraction data, however the toluene model is clearly a better fit to the observed electron density. A contour map of Fo showing the toluene model overlayed with the electron density is given in Figure S6.

Plane: 0.6338x-22.2843y 0.9207z = -0.8864 Cont-Lev(eA-3): -0.60 4.00 0.20 Fo-Map
Tol = 1.5 Ang Step = 0.3000 Ang Resolution 18.7 Deg. Omtt 2*SLgI

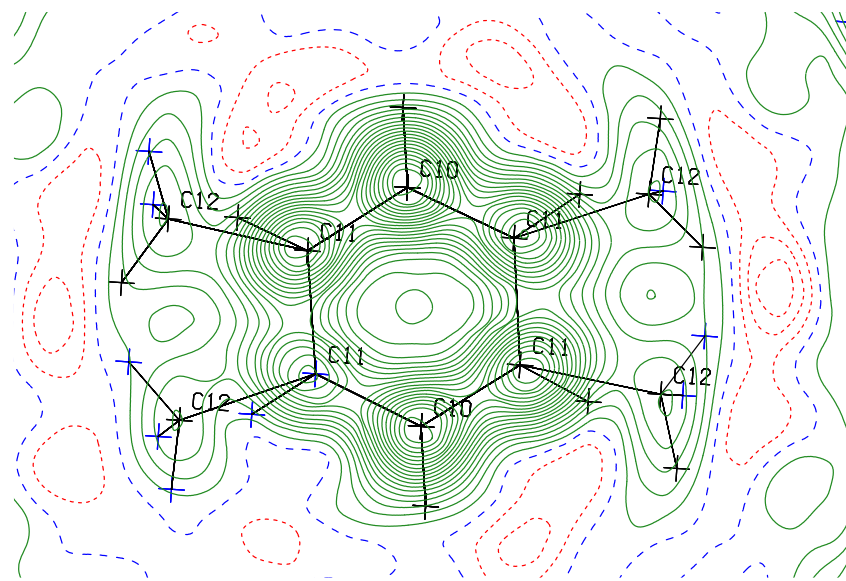


Figure S6. Electron density contour map of **5-Li** modeled as a disordered toluene molecule, **6-Li**.

$R_1 = 0.061$, $wR_2 0.172$

General methods. Structure refinement was performed using Olex2² with the ShelXL refinement package.³ Electron density contour maps were generated using PLATON.⁴ A CIF file containing both the **5-Li** and **6-Li** model and the tabulated hklf3 structure files is attached as supporting information.

Table S1. Crystal data and structure refinement for **6-K**.

Identification code	20047z_a
Empirical formula	C48.50 H100 K N4 Si8 Ti2
Formula weight	1098.94
Temperature	126(2) K
Wavelength	0.71073 Å
Crystal system	Monoclinic
Space group	P2 ₁ /c
Unit cell dimensions	$a = 17.4417(7)$ Å $a = 90^\circ$ $b = 25.7154(9)$ Å $b = 106.8550(10)^\circ$ $c = 14.5174(5)$ Å $g = 90^\circ$
Volume	6231.6(4) Å ³
Z	4
Density (calculated)	1.171 Mg/m ³
Absorption coefficient	0.510 mm ⁻¹
$F(000)$	2376
Crystal color, morphology	purple, Block
Crystal size	0.400 x 0.300 x 0.200 mm ³
Theta range for data collection	1.999 to 26.060°
Index ranges	-21 ≤ h ≤ 21, -31 ≤ k ≤ 31, -17 ≤ l ≤ 17
Reflections collected	129122
Independent reflections	12306 [$R(\text{int}) = 0.1044$]
Observed reflections	8721
Completeness to theta = 25.242°	99.9%
Absorption correction	Multi-scan
Refinement method	Full-matrix least-squares on F^2
Data / restraints / parameters	12306 / 21 / 683
Goodness-of-fit on F^2	1.060
Final R indices [$I > 2\sigma(I)$]	$R_1 = 0.0406$, $wR_2 = 0.0840$
R indices (all data)	$R_1 = 0.0745$, $wR_2 = 0.0970$
Largest diff. peak and hole	0.364 and -0.290 e.Å ⁻³

Table S2. Selected bond lengths [Å] and angles [°] for **6-K**.

Ti(1)-N(2)	2.129(2)	C(5)-H(5)	0.96(3)
Ti(1)-N(1)	2.147(2)	C(4)-C(3)	1.446(4)
Ti(1)-C(5)	2.227(3)	C(4)-H(4)	0.89(3)
Ti(1)-C(4)	2.245(3)	C(3)-C(2)	1.449(4)
Ti(1)-C(2)	2.256(3)	C(3)-H(3)	0.98(3)
Ti(1)-C(1)	2.345(3)	C(2)-H(2)	0.92(3)
Ti(1)-C(3)	2.440(3)		
Ti(1)-C(6)	2.453(3)	N(2)-Ti(1)-N(1)	103.82(8)
Ti(1)-K(1)	3.7203(7)	N(2)-Ti(1)-C(5)	104.81(9)
Ti(2)-N(3)	2.028(2)	N(1)-Ti(1)-C(5)	130.01(9)
Ti(2)-N(4)	2.030(2)	N(2)-Ti(1)-C(4)	139.04(9)
Ti(2)-C(3)	2.189(3)	N(1)-Ti(1)-C(4)	97.82(9)
Ti(2)-C(6)	2.205(3)	C(5)-Ti(1)-C(4)	37.52(9)
Ti(2)-C(4)	2.322(3)	N(2)-Ti(1)-C(2)	135.63(9)
Ti(2)-C(5)	2.356(3)	N(1)-Ti(1)-C(2)	106.97(9)
Ti(2)-C(1)	2.368(3)	C(5)-Ti(1)-C(2)	78.43(10)
Ti(2)-C(2)	2.395(3)	C(4)-Ti(1)-C(2)	66.18(10)
K(1)-N(1)	2.904(2)	N(2)-Ti(1)-C(1)	103.56(8)
K(1)-N(2)	2.960(2)	N(1)-Ti(1)-C(1)	142.24(9)
K(1)-C(34)	3.226(3)	C(5)-Ti(1)-C(1)	65.36(10)
K(1)-C(33)	3.234(3)	C(4)-Ti(1)-C(1)	77.49(10)
K(1)-C(35)	3.308(3)	C(2)-Ti(1)-C(1)	36.58(9)
K(1)-C(32)	3.352(3)	N(2)-Ti(1)-C(3)	165.34(9)
K(1)-C(14)	3.372(3)	N(1)-Ti(1)-C(3)	90.84(8)
K(1)-C(36)	3.392(3)	C(5)-Ti(1)-C(3)	64.52(9)
K(1)-C(37)	3.402(3)	C(4)-Ti(1)-C(3)	35.65(9)
K(1)-C(12)	3.408(3)	C(2)-Ti(1)-C(3)	35.66(9)
C(7)-C(1)	1.508(4)	C(1)-Ti(1)-C(3)	63.40(9)
C(7)-H(7A)	0.9800	N(2)-Ti(1)-C(6)	93.59(8)
C(7)-H(7B)	0.9800	N(1)-Ti(1)-C(6)	161.09(9)
C(7)-H(7C)	0.9800	C(5)-Ti(1)-C(6)	35.30(9)
C(1)-C(6)	1.436(4)	C(4)-Ti(1)-C(6)	63.68(9)
C(1)-C(2)	1.446(4)	C(2)-Ti(1)-C(6)	63.26(9)
C(6)-C(5)	1.435(4)	C(1)-Ti(1)-C(6)	34.73(9)
C(6)-H(6)	0.89(3)	C(3)-Ti(1)-C(6)	71.89(9)
C(5)-C(4)	1.438(4)	N(2)-Ti(1)-K(1)	52.64(6)

N(1)-Ti(1)-K(1)	51.18(6)	N(1)-K(1)-C(34)	121.19(7)
C(5)-Ti(1)-K(1)	136.92(7)	N(2)-K(1)-C(34)	168.76(7)
C(4)-Ti(1)-K(1)	135.76(7)	N(1)-K(1)-C(33)	133.10(7)
C(2)-Ti(1)-K(1)	144.40(7)	N(2)-K(1)-C(33)	147.70(8)
C(1)-Ti(1)-K(1)	146.71(6)	C(34)-K(1)-C(33)	24.85(9)
C(3)-Ti(1)-K(1)	142.01(6)	N(1)-K(1)-C(35)	126.45(8)
C(6)-Ti(1)-K(1)	145.53(7)	N(2)-K(1)-C(35)	149.62(8)
N(3)-Ti(2)-N(4)	107.88(9)	C(34)-K(1)-C(35)	24.20(8)
N(3)-Ti(2)-C(3)	121.14(10)	C(33)-K(1)-C(35)	42.85(9)
N(4)-Ti(2)-C(3)	111.62(9)	N(1)-K(1)-C(32)	156.12(7)
N(3)-Ti(2)-C(6)	112.99(10)	N(2)-K(1)-C(32)	126.58(7)
N(4)-Ti(2)-C(6)	120.36(9)	C(34)-K(1)-C(32)	43.20(8)
C(3)-Ti(2)-C(6)	81.65(10)	C(33)-K(1)-C(32)	24.43(8)
N(3)-Ti(2)-C(4)	94.53(9)	C(35)-K(1)-C(32)	49.53(8)
N(4)-Ti(2)-C(4)	148.85(9)	N(1)-K(1)-C(14)	113.53(6)
C(3)-Ti(2)-C(4)	37.25(10)	N(2)-K(1)-C(14)	56.26(6)
C(6)-Ti(2)-C(4)	66.53(10)	C(34)-K(1)-C(14)	115.36(8)
N(3)-Ti(2)-C(5)	91.80(10)	C(33)-K(1)-C(14)	91.47(8)
N(4)-Ti(2)-C(5)	156.07(9)	C(35)-K(1)-C(14)	119.61(8)
C(3)-Ti(2)-C(5)	66.55(10)	C(32)-K(1)-C(14)	73.11(7)
C(6)-Ti(2)-C(5)	36.49(9)	N(1)-K(1)-C(36)	145.64(7)
C(4)-Ti(2)-C(5)	35.80(9)	N(2)-K(1)-C(36)	128.44(7)
N(3)-Ti(2)-C(1)	149.31(9)	C(34)-K(1)-C(36)	42.17(8)
N(4)-Ti(2)-C(1)	93.81(9)	C(33)-K(1)-C(36)	48.99(8)
C(3)-Ti(2)-C(1)	66.87(9)	C(35)-K(1)-C(36)	23.87(8)
C(6)-Ti(2)-C(1)	36.37(9)	C(32)-K(1)-C(36)	41.67(8)
C(4)-Ti(2)-C(1)	75.55(9)	C(14)-K(1)-C(36)	99.99(8)
C(5)-Ti(2)-C(1)	63.05(9)	N(1)-K(1)-C(37)	168.24(7)
N(3)-Ti(2)-C(2)	156.59(9)	N(2)-K(1)-C(37)	119.74(7)
N(4)-Ti(2)-C(2)	91.53(9)	C(34)-K(1)-C(37)	49.05(8)
C(3)-Ti(2)-C(2)	36.49(9)	C(33)-K(1)-C(37)	41.85(8)
C(6)-Ti(2)-C(2)	64.96(10)	C(35)-K(1)-C(37)	41.81(8)
C(4)-Ti(2)-C(2)	62.76(9)	C(32)-K(1)-C(37)	23.41(7)
C(5)-Ti(2)-C(2)	73.23(10)	C(14)-K(1)-C(37)	78.20(7)
C(1)-Ti(2)-C(2)	35.34(9)	C(36)-K(1)-C(37)	23.41(7)
N(1)-K(1)-N(2)	70.03(6)	N(1)-K(1)-C(12)	56.16(6)

N(2)-K(1)-C(12)	114.21(6)	C(14)-K(1)-C(12)	169.33(7)
C(34)-K(1)-C(12)	74.74(8)	C(36)-K(1)-C(12)	89.93(8)
C(33)-K(1)-C(12)	98.06(8)	C(37)-K(1)-C(12)	112.17(8)
C(35)-K(1)-C(12)	70.98(8)		
C(32)-K(1)-C(12)	117.38(8)		

Table S3. Crystal data and structure refinement for **6-Li**.

Identification code	123vgya
Empirical formula	C43 H109 Li N8 Si8 Ti2
Formula weight	1065.84
Temperature	126(2) K
Wavelength	1.54178 Å
Crystal system	Orthorhombic
Space group	I222
Unit cell dimensions	$a = 11.4958(13)$ Å $a = 90^\circ$. $b = 13.0602(15)$ Å $b = 90^\circ$. $c = 22.084(3)$ Å $g = 90^\circ$.
Volume	3315.7(7) Å ³
Z	2
Density (calculated)	1.068 Mg/m ³
Absorption coefficient	3.673 mm ⁻¹
F(000)	1164
Crystal size	0.100 x 0.050 x 0.050 mm ³
Theta range for data collection	3.932 to 74.914°.
Index ranges	-13≤h≤14, -16≤k≤16, -26≤l≤27
Reflections collected	36985
Independent reflections	3408 [R(int) = 0.0985]
Completeness to theta = 67.679°	99.6 %
Max. and min. transmission	0.7538 and 0.5941
Refinement method	Full-matrix least-squares on F ²
Data / restraints / parameters	3408 / 0 / 189
Goodness-of-fit on F ²	1.048
Final R indices [I>2sigma(I)]	R1 = 0.0519, wR2 = 0.1223
R indices (all data)	R1 = 0.0688, wR2 = 0.1320
Absolute structure parameter	0.042(17)
Largest diff. peak and hole	0.378 and -0.615 e.Å ⁻³

Table S4. Selected bond lengths [\AA] and angles [$^\circ$] for **6-Li**.

Ti(1)-N(1)#1	2.063(4)	C(2)#2-C(1)-Ti(1)#3	69.0(3)
Ti(1)-N(1)	2.063(4)	C(2)-C(1)-Ti(1)	69.0(3)
N(2)-Li(1)	2.128(5)	C(2)#2-C(1)-Ti(1)	76.7(3)
C(1)-C(2)	1.421(6)	Ti(1)#3-C(1)-Ti(1)	105.0(3)
C(1)-C(2)#2	1.421(6)	C(1)-C(2)-C(2)#3	117.7(3)
C(1)-Ti(1)#3	2.303(4)	C(1)-C(2)-C(3)	132.6(9)
C(2)-C(2)#3	1.449(12)	C(2)#3-C(2)-C(3)	104.7(8)
C(2)-C(3)	1.61(2)	C(1)-C(2)-Ti(1)	74.5(3)
C(2)-Ti(1)#3	2.411(7)	C(2)#3-C(2)-Ti(1)	78.7(4)
Li(1)-N(2)#1	2.128(5)	C(3)-C(2)-Ti(1)	137.3(10)
Li(1)-N(2)#4	2.128(5)	C(1)-C(2)-Ti(1)#3	68.3(3)
Li(1)-N(2)#5	2.128(5)	C(2)#3-C(2)-Ti(1)#3	65.2(5)
		C(3)-C(2)-Ti(1)#3	116.4(11)
N(1)#1-Ti(1)-N(1)	107.2(3)	Ti(1)-C(2)-Ti(1)#3	103.74(19)
Si(1)-N(1)-Ti(1)	123.0(2)	N(2)-Li(1)-N(2)#1	112.9(3)
Si(2)-N(1)-Ti(1)	117.2(2)	N(2)-Li(1)-N(2)#4	86.9(3)
C(11)-N(2)-Li(1)	114.5(4)	N(2)#1-Li(1)-N(2)#4	131.6(3)
C(10)-N(2)-Li(1)	112.4(4)	N(2)-Li(1)-N(2)#5	131.6(3)
C(12)-N(2)-Li(1)	101.6(4)	N(2)#1-Li(1)-N(2)#5	86.9(3)
C(2)-C(1)-C(2)#2	122.2(6)	N(2)#4-Li(1)-N(2)#5	112.9(3)
C(2)-C(1)-Ti(1)#3	76.7(3)		

Table S5. Crystal data and structure refinement for 7.

Identification code	21120a
Empirical formula	C14 H39 Cl N4 O0.50 Si2 Ti
Formula weight	411.02
Temperature	126.0 K
Wavelength	1.54178 Å
Crystal system	Monoclinic
Space group	P 1 21/c 1
Unit cell dimensions	$a = 13.0154(5)$ Å $a = 90^\circ$. $b = 26.2836(10)$ Å $b = 114.484(2)^\circ$. $c = 14.8634(6)$ Å $g = 90^\circ$.
Volume	4627.4(3) Å ³
Z	8
Density (calculated)	1.180 Mg/m ³
Absorption coefficient	5.222 mm ⁻¹
F(000)	1776
Crystal size	0.1 x 0.1 x 0.1 mm ³
Theta range for data collection	3.363 to 70.187°.
Index ranges	-15≤h≤15, -32≤k≤32, -18≤l≤18
Reflections collected	95008
Independent reflections	8777 [R(int) = 0.0877]
Completeness to theta = 67.679°	99.9 %
Absorption correction	Semi-empirical from equivalents
Max. and min. transmission	0.7533 and 0.3741
Refinement method	Full-matrix least-squares on F ²
Data / restraints / parameters	8777 / 0 / 412
Goodness-of-fit on F ²	1.101
Final R indices [I>2sigma(I)]	R1 = 0.0901, wR2 = 0.2073
R indices (all data)	R1 = 0.1097, wR2 = 0.2187
Largest diff. peak and hole	1.025 and -1.400 e.Å ⁻³

Table S6. Bond lengths [Å] and angles [°] for 7.

Ti(1)-Cl(1)	2.3913(18)	N(3)-Ti(1)-N(5)	151.8(2)
Ti(1)-N(1)	1.767(5)	N(3)-Ti(1)-N(4)	92.2(2)
Ti(1)-N(3)	2.011(6)	N(5)-Ti(1)-Cl(1)	85.17(17)
Ti(1)-N(5)	2.298(6)	N(5)-Ti(1)-N(4)	76.2(2)
Ti(1)-N(4)	2.344(6)	N(4)-Ti(1)-Cl(1)	153.97(17)
Ti(2)-Cl(2)	2.3894(18)	N(2)-Ti(2)-Cl(2)	102.43(17)
Ti(2)-N(2)	1.766(5)	N(2)-Ti(2)-N(8)	94.6(2)
Ti(2)-N(8)	2.306(6)	N(2)-Ti(2)-N(6)	112.6(2)
Ti(2)-N(6)	2.020(6)	N(2)-Ti(2)-N(7)	96.9(2)
Ti(2)-N(7)	2.358(5)	N(8)-Ti(2)-Cl(2)	85.76(16)
N(1)-Ti(1)-Cl(1)	103.46(17)	N(8)-Ti(2)-N(7)	76.9(2)
N(1)-Ti(1)-N(3)	111.9(2)	N(6)-Ti(2)-Cl(2)	96.32(16)
N(1)-Ti(1)-N(5)	95.0(2)	N(6)-Ti(2)-N(8)	151.4(2)
N(1)-Ti(1)-N(4)	96.2(2)	N(6)-Ti(2)-N(7)	90.6(2)
N(3)-Ti(1)-Cl(1)	96.02(16)	N(7)-Ti(2)-Cl(2)	154.97(16)

Table S7. Crystal data and structure refinement for **8**.

Identification code	21072_abs	
Empirical formula	C24 H72 K2 N6 Si8 Ti2	
Formula weight	843.59	
Temperature	396(2) K	
Wavelength	0.71073 Å	
Crystal system	Monoclinic	
Space group	P2 ₁ /n	
Unit cell dimensions	a = 9.367(4) Å	a= 90°.
	b = 14.742(5) Å	b= 90.117(6)°.
	c = 16.488(6) Å	g = 90°.
Volume	2276.7(15) Å ³	
Z	2	
Density (calculated)	1.231 Mg/m ³	
Absorption coefficient	0.768 mm ⁻¹	
F(000)	904	
Crystal size	0.263 x 0.162 x 0.075 mm ³	
Theta range for data collection	1.853 to 25.483°.	
Index ranges	-10<=h<=11, -17<=k<=17, -19<=l<=17	
Reflections collected	11137	
Independent reflections	4168 [R(int) = 0.0518]	
Completeness to theta = 25.483°	98.5 %	
Absorption correction	Semi-empirical from equivalents	
Max. and min. transmission	0.7452 and 0.6443	
Refinement method	Full-matrix least-squares on F ²	
Data / restraints / parameters	4168 / 0 / 334	
Goodness-of-fit on F ²	1.005	
Final R indices [I>2sigma(I)]	R1 = 0.0439, wR2 = 0.0978	
R indices (all data)	R1 = 0.0684, wR2 = 0.1107	
Largest diff. peak and hole	0.426 and -0.357 e.Å ⁻³	

Table S8. Selected bond lengths [Å] and angles [°] for **8**.

Ti(1)-N(3)	2.073(3)	C(7)-Si(3)-K(1)	81.59(18)
Ti(1)-N(1)#1	1.825(3)	C(8)-Si(3)-K(1)	74.10(15)
Ti(1)-N(1)	1.836(3)	N(3)-Si(4)-K(1)	52.39(9)
Ti(1)-N(2)#1	2.091(3)	C(12)-Si(4)-K(1)	119.55(13)
K(1)-N(3)	2.993(3)	C(10)-Si(4)-K(1)	133.99(15)
K(1)-N(1)	2.831(3)	C(11)-Si(4)-K(1)	59.58(15)
K(1)-N(2)	2.976(3)	N(2)-Si(1)-K(1)	56.97(9)
N(1)-Ti(1)#1	1.825(3)	C(1)-Si(1)-K(1)	149.33(15)
N(2)-Ti(1)#1	2.091(3)	C(2)-Si(1)-K(1)	105.33(19)
C(9)-K(1)#2	3.424(4)	C(3)-Si(1)-K(1)	60.15(13)
		Ti(1)-N(3)-K(1)	85.11(9)
N(3)-Ti(1)-N(2)#1	116.95(11)	Si(3)-N(3)-Ti(1)	118.28(14)
N(1)#1-Ti(1)-N(3)	114.06(11)	Si(4)-N(3)-Ti(1)	122.51(14)
N(1)-Ti(1)-N(3)	109.50(11)	Si(4)-N(3)-K(1)	100.32(11)
N(1)#1-Ti(1)-N(1)	86.33(12)	Ti(1)#1-N(1)-Ti(1)	93.67(12)
N(1)-Ti(1)-N(2)#1	117.77(11)	Ti(1)-N(1)-K(1)	94.44(10)
N(1)#1-Ti(1)-N(2)#1	108.38(11)	Ti(1)#1-N(1)-K(1)	94.15(10)
N(3)-Si(3)-K(1)	58.65(9)	Ti(1)#1-N(2)-K(1)	84.77(9)
C(9)-Si(3)-K(1)	171.01(17)		

Table S9. Crystal data and structure refinement for **8·THF**.

Identification code	21037_abs2
Empirical formula	C16 H44 K N3 O Si4 Ti
Formula weight	493.90
Temperature	125.0 K
Wavelength	0.71073 Å
Crystal system	Monoclinic
Space group	P 1 21/c 1
Unit cell dimensions	 $a = 10.4873(4)$ Å $a = 90^\circ$. $b = 21.2094(7)$ Å $b = 107.2060(10)^\circ$. $c = 12.8048(5)$ Å $g = 90^\circ$.
Volume	2720.70(17) Å ³
Z	4
Density (calculated)	1.206 Mg/m ³
Absorption coefficient	0.655 mm ⁻¹
F(000)	1064
Crystal size	0.1 x 0.1 x 0.05 mm ³
Theta range for data collection	2.248 to 29.616°.
Index ranges	-14≤h≤14, -29≤k≤29, -17≤l≤17
Reflections collected	79275
Independent reflections	7655 [R(int) = 0.0691]
Completeness to theta = 25.242°	99.8 %
Absorption correction	None
Max. and min. transmission	0.7459 and 0.6822
Refinement method	Full-matrix least-squares on F ²
Data / restraints / parameters	7655 / 0 / 265
Goodness-of-fit on F ²	1.067
Final R indices [I>2sigma(I)]	R1 = 0.0321, wR2 = 0.0725
R indices (all data)	R1 = 0.0513, wR2 = 0.0812
Largest diff. peak and hole	0.412 and -0.300 e.Å ⁻³

Table S10. Selected bond lengths [Å] and angles [°] for **8**·THF.

Ti(1)-N(2)	2.0753(13)	C(7)-Si(3)-K(1)	150.52(6)
Ti(1)-N(1)	1.8239(13)	Ti(1)-N(2)-K(1)#1	85.23(4)
Ti(1)-N(1)#1	1.8354(13)	Si(2)-N(2)-Ti(1)	118.30(7)
Ti(1)-N(3)	2.0942(13)	Si(2)-N(2)-K(1)#1	91.35(5)
K(1)-N(1)	2.8655(13)	Si(1)-N(2)-Ti(1)	122.17(7)
K(1)-O(1)	2.6629(14)	Si(1)-N(2)-K(1)#1	101.58(5)
N(2)-K(1)#1	2.9989(13)	Ti(1)-N(1)-Ti(1)#1	93.69(6)
N(1)-Ti(1)#1	1.8354(13)	Ti(1)-N(1)-K(1)	93.50(5)
		Ti(1)#1-N(1)-K(1)	93.73(5)
N(2)-Ti(1)-N(3)	116.47(5)	Ti(1)-N(3)-K(1)	84.95(4)
N(1)-Ti(1)-N(2)	114.14(5)	Si(4)-N(3)-Ti(1)	122.94(7)
N(1)#1-Ti(1)-N(2)	109.95(6)	Si(4)-N(3)-K(1)	106.74(6)
N(1)-Ti(1)-N(1)#1	86.31(6)	Si(3)-N(3)-Ti(1)	115.74(7)
N(1)-Ti(1)-N(3)	108.82(6)	Si(3)-N(3)-K(1)	95.89(5)
N(1)#1-Ti(1)-N(3)	117.46(5)	Si(3)-N(3)-Si(4)	118.07(7)
O(1)-K(1)-N(1)	166.74(5)	C(13)-O(1)-K(1)	120.46(13)
N(3)-Si(4)-K(1)	47.76(4)	C(16B)-O(1)-K(1)	135.63(16)
C(11)-Si(4)-K(1)	75.85(6)	C(16A)-O(1)-K(1)	121.3(3)
C(10)-Si(4)-K(1)	96.24(6)	K(1)-C(9)-H(9A)	66.5
C(12)-Si(4)-K(1)	155.73(6)	K(1)-C(9)-H(9B)	163.2
N(2)-Si(2)-K(1)#1	59.02(4)	K(1)-C(9)-H(9C)	59.7
C(6)-Si(2)-K(1)#1	80.19(6)	Si(3)-C(9)-K(1)	86.90(6)
C(4)-Si(2)-K(1)#1	75.24(6)	K(1)#1-C(4)-H(4A)	38.6
C(5)-Si(2)-K(1)#1	173.21(6)	K(1)#1-C(4)-H(4B)	136.8
N(2)-Si(1)-K(1)#1	51.53(4)	K(1)#1-C(4)-H(4C)	109.5
C(2)-Si(1)-K(1)#1	118.64(5)	Si(2)-C(4)-K(1)#1	73.63(6)
C(3)-Si(1)-K(1)#1	135.66(6)	K(1)#1-C(1)-H(1A)	70.4
C(1)-Si(1)-K(1)#1	61.23(6)	K(1)#1-C(1)-H(1B)	160.0
N(3)-Si(3)-K(1)	55.48(5)	K(1)#1-C(1)-H(1C)	54.4
C(9)-Si(3)-K(1)	61.56(6)	Si(1)-C(1)-K(1)#1	88.67(6)
C(8)-Si(3)-K(1)	104.89(6)		

Table S11. Crystal data and structure refinement for **9**.

Identification code	22052b
Empirical formula	C ₃₀ H ₇₇ KN ₃ O ₆ Si ₆ Ti
Formula weight	831.48
Temperature	150.0 K
Wavelength	0.71073 Å
Crystal system	Monoclinic
Space group	P 1 21/c 1
Unit cell dimensions	a = 23.2036(6) Å b = 20.0225(5) Å c = 22.5981(4) Å
Volume	9620.3(4) Å ³
Z	8
Density (calculated)	1.148 Mg/m ³
Absorption coefficient	0.450 mm ⁻¹
F(000)	3608
Crystal size	0.1 x 0.1 x 0.1 mm ³
Theta range for data collection	1.916 to 28.312°.
Index ranges	-30<=h<=22, -21<=k<=26, -29<=l<=30
Reflections collected	85817
Independent reflections	23870 [R(int) = 0.0622]
Completeness to theta = 25.242°	99.9 %
Absorption correction	None
Max. and min. transmission	0.7457 and 0.6670
Refinement method	Full-matrix least-squares on F ²
Data / restraints / parameters	23870 / 0 / 881
Goodness-of-fit on F ²	1.014
Final R indices [I>2sigma(I)]	R1 = 0.0525, wR2 = 0.1022
R indices (all data)	R1 = 0.0955, wR2 = 0.1181
Largest diff. peak and hole	0.349 and -0.357 e.Å ⁻³

Table S12. Selected bond lengths [\AA] and angles [$^\circ$] for **9**.

Ti(1)-Si(1)	2.7614(8)	N(4)-Ti(2)-Si(7)	38.66(6)
Ti(1)-N(1)	2.0059(19)	N(4)-Ti(2)-N(5)	127.13(8)
Ti(1)-N(2)	2.059(2)	N(4)-Ti(2)-N(6)	107.17(8)
Ti(1)-N(3)	2.0305(18)	N(4)-Ti(2)-C(31)	79.87(8)
Ti(1)-C(1)	2.215(2)	N(5)-Ti(2)-Si(7)	117.68(6)
Ti(2)-Si(7)	2.7637(8)	N(5)-Ti(2)-N(6)	114.18(8)
Ti(2)-N(4)	2.004(2)	N(5)-Ti(2)-C(31)	98.12(9)
Ti(2)-N(5)	2.0293(19)	N(6)-Ti(2)-Si(7)	128.05(6)
Ti(2)-N(6)	2.050(2)	N(6)-Ti(2)-C(31)	128.10(8)
Ti(2)-C(31)	2.223(2)	C(31)-Ti(2)-Si(7)	41.31(7)
K(2)-O(11)	2.8155(18)	O(11)-K(2)-O(7)	114.25(5)
K(2)-O(7)	2.8427(19)	O(11)-K(2)-O(10)	60.00(5)
K(2)-O(12)	2.7855(17)	O(11)-K(2)-O(9)	116.11(5)
K(2)-O(10)	2.8211(19)	O(11)-K(2)-O(8)	160.01(6)
K(2)-O(9)	2.8375(18)	O(7)-K(2)-O(8)	58.28(5)
K(2)-O(8)	2.8619(19)	O(12)-K(2)-O(11)	59.81(5)
K(1)-O(5)	2.8280(18)	O(12)-K(2)-O(7)	59.35(6)
K(1)-O(3)	2.8690(17)	O(12)-K(2)-O(10)	119.79(5)
K(1)-O(4)	2.7935(17)	O(12)-K(2)-O(9)	160.62(6)
K(1)-O(6)	2.8091(16)	O(12)-K(2)-O(8)	117.53(6)
K(1)-O(2)	2.8696(18)	O(10)-K(2)-O(7)	156.19(6)
K(1)-O(1)	2.7924(18)	O(10)-K(2)-O(9)	59.33(5)
C(1)-K(2)#1	3.258(2)	O(10)-K(2)-O(8)	118.24(6)
		O(9)-K(2)-O(7)	112.73(6)
N(1)-Ti(1)-Si(1)	38.71(6)	O(9)-K(2)-O(8)	58.93(5)
N(1)-Ti(1)-N(2)	108.55(8)	O(5)-K(1)-O(3)	114.86(5)
N(1)-Ti(1)-N(3)	126.25(8)	O(5)-K(1)-O(2)	159.83(5)
N(1)-Ti(1)-C(1)	80.05(8)	O(3)-K(1)-O(2)	58.21(5)
N(2)-Ti(1)-Si(1)	125.64(6)	O(4)-K(1)-O(5)	59.47(5)
N(2)-Ti(1)-C(1)	125.77(8)	O(4)-K(1)-O(3)	59.00(5)
N(3)-Ti(1)-Si(1)	120.27(6)	O(4)-K(1)-O(6)	119.12(5)
N(3)-Ti(1)-N(2)	113.85(8)	O(4)-K(1)-O(2)	117.21(5)
N(3)-Ti(1)-C(1)	99.59(9)	O(6)-K(1)-O(5)	59.77(5)
C(1)-Ti(1)-Si(1)	41.34(7)	O(6)-K(1)-O(3)	157.01(5)

O(6)-K(1)-O(2)	118.10(5)	C(53)-O(9)-K(2)	113.36(16)
O(1)-K(1)-O(5)	114.87(5)	C(30)-O(1)-K(1)	117.46(15)
O(1)-K(1)-O(3)	111.91(5)	C(19)-O(1)-K(1)	113.95(14)
O(1)-K(1)-O(4)	155.61(6)	C(51)-O(8)-K(2)	117.43(15)
O(1)-K(1)-O(6)	59.27(5)	C(50)-O(8)-K(2)	117.86(15)
O(1)-K(1)-O(2)	58.84(5)	Si(2)-N(1)-Ti(1)	137.82(11)
C(27)-O(5)-K(1)	108.71(14)	Si(2)-N(1)-Si(1)	125.89(12)
C(26)-O(5)-K(1)	111.64(14)	Si(1)-N(1)-Ti(1)	94.92(9)
C(23)-O(3)-K(1)	111.92(14)	Si(4)-N(2)-Ti(1)	119.68(9)
C(22)-O(3)-K(1)	113.92(15)	Si(3)-N(2)-Ti(1)	121.71(10)
C(24)-O(4)-K(1)	119.23(15)	Si(7)-N(4)-Ti(2)	95.11(9)
C(25)-O(4)-K(1)	118.20(14)	Si(8)-N(4)-Ti(2)	136.35(11)
C(28)-O(6)-K(1)	117.38(13)	Si(6)-N(3)-Ti(1)	123.02(11)
C(29)-O(6)-K(1)	115.69(15)	Si(5)-N(3)-Ti(1)	116.24(10)
C(56)-O(11)-K(2)	112.10(14)	Si(9)-N(5)-Ti(2)	122.91(11)
C(57)-O(11)-K(2)	109.63(15)	Si(10)-N(5)-Ti(2)	113.49(10)
C(21)-O(2)-K(1)	118.00(15)	Si(12)-N(6)-Ti(2)	120.81(11)
C(20)-O(2)-K(1)	117.47(14)	Si(11)-N(6)-Ti(2)	120.22(10)
C(49)-O(7)-K(2)	116.20(15)	Ti(2)-C(31)-K(1)	172.56(11)
C(60)-O(7)-K(2)	114.14(16)	Si(7)-C(31)-Ti(2)	85.41(9)
C(58)-O(12)-K(2)	118.51(15)	Si(7)-C(31)-K(1)	92.35(9)
C(59)-O(12)-K(2)	119.12(16)	Ti(1)-C(1)-K(2)#1	172.53(11)
C(55)-O(10)-K(2)	115.84(14)	Si(1)-C(1)-Ti(1)	85.55(10)
C(54)-O(10)-K(2)	117.00(16)	Si(1)-C(1)-K(2)#1	92.51(9)
C(52)-O(9)-K(2)	111.34(15)	Si(3)-C(8)-K(1)	165.57(12)

Table S13. Crystal data and structure refinement for **10**.

Identification code	22004a	
Empirical formula	C32 H88 N6 O2 Si8 Ti2	
Formula weight	909.60	
Temperature	150(2) K	
Wavelength	0.71073 Å	
Crystal system	Monoclinic	
Space group	P2 ₁ /n	
Unit cell dimensions	a = 10.6293(16) Å	a= 90°.
	b = 24.141(3) Å	b= 113.538(4)°.
	c = 11.2893(12) Å	g = 90°.
Volume	2655.8(6) Å ³	
Z	2	
Density (calculated)	1.137 Mg/m ³	
Absorption coefficient	0.512 mm ⁻¹	
F(000)	988	
Crystal size	0.1 x 0.1 x 0.1 mm ³	
Theta range for data collection	2.226 to 30.632°.	
Index ranges	-15<=h<=11, -34<=k<=27, -15<=l<=16	
Reflections collected	28586	
Independent reflections	8158 [R(int) = 0.0364]	
Completeness to theta = 25.242°	99.9 %	
Absorption correction	Semi-empirical from equivalents	
Max. and min. transmission	0.7461 and 0.6507	
Refinement method	Full-matrix least-squares on F ²	
Data / restraints / parameters	8158 / 0 / 287	
Goodness-of-fit on F ²	1.028	
Final R indices [I>2sigma(I)]	R1 = 0.0381, wR2 = 0.0894	
R indices (all data)	R1 = 0.0574, wR2 = 0.0980	
Largest diff. peak and hole	0.487 and -0.298 e.Å ⁻³	

Table S14. Selected bond lengths [\AA] and angles [$^\circ$] for **10**.

Ti(1)-N(1)	1.7625(12)	N(3)-Ti(1)-O(1)	123.16(5)
Ti(1)-N(2)	1.9951(13)	C(16)-O(1)-Ti(1)	127.25(10)
Ti(1)-N(3)	2.0107(12)	C(13)-O(1)-Ti(1)	122.29(10)
Ti(1)-O(1)	2.0931(11)	N(1)#1-N(1)-Ti(1)	174.11(14)
N(1)-N(1)#1	1.276(2)	Si(4B)-N(3)-Ti(1)	118.11(9)
		Si(3)-N(3)-Ti(1)	121.82(7)
N(1)-Ti(1)-N(2)	111.49(6)	Si(4A)-N(3)-Ti(1)	114.44(13)
N(1)-Ti(1)-N(3)	108.72(5)	Si(2)-N(2)-Ti(1)	117.82(7)
N(2)-Ti(1)-N(3)	115.43(5)	Si(1)-N(2)-Ti(1)	121.86(7)
N(1)-Ti(1)-O(1)	96.12(5)		
N(2)-Ti(1)-O(1)	100.22(5)		

Table S15. Selected bond distance ranges (\AA) and angles ($^\circ$) of the Ti-arene moiety of **1**,⁵ **2**,⁶ **3**,⁷

4,⁸ **6-K**, and **6-Li**.

	1 ⁵	2 ⁶	3 ⁷	4 ⁸	6-K (this work)	6-Li (this work)
Ti ₁ -C ₁	2.418(3)	2.354(4)	2.347(4)	2.318(1)	2.345(2)	2.231(7)
Ti ₁ -C ₂	2.233(4)	2.142(4)	2.394(4)	2.285(1)	2.256(3)	2.303(4)
Ti ₁ -C ₃	2.368(3)	2.379(3)	2.307(3)	2.262(1)	2.440(3)	2.412(7)
Ti ₁ -C ₄	2.351(3)	2.339(3)	2.207(4)	2.281(1)	2.245(3)	2.231(7)
Ti ₁ -C ₅	2.202(4)	2.151(4)	2.353(5)	2.316(1)	2.227(3)	2.303(4)
Ti ₁ -C ₆	2.390(3)	2.321(4)	2.307(3)	2.223(1)	2.454(3)	2.412(7)
Ti ₂ -C ₁			2.327(5)	2.281(1)	2.368(3)	2.412(7)
Ti ₂ -C ₂			2.237(5)	2.316(1)	2.395(3)	2.303(4)
Ti ₂ -C ₃			2.222(5)	2.223(1)	2.189(3)	2.231(7)
Ti ₂ -C ₄			2.300(4)	2.318(1)	2.322(3)	2.412(7)
Ti ₂ -C ₅			2.188(4)	2.285(1)	2.356(3)	2.303(4)
Ti ₂ -C ₆			2.299(3)	2.262(1)	2.205(3)	2.231(7)
Ti-C _{ave}	2.32(9)	2.3(1)	2.29(6)	2.28(3)	2.32(6)	2.32(8)
C ₁ -C ₂	1.442(5)	1.475(5)	1.425(5)	1.490(1)	1.446(4)	1.448(8)
C ₂ -C ₃	1.433(6)	1.490(5)	1.440(5)	1.472(2)	1.449(4)	1.422(6)
C ₃ -C ₄	1.357(7)	1.388(5)	1.420(6)	1.474(1)	1.446(4)	1.422(6)
C ₄ -C ₅	1.429(5)	1.447(5)	1.427(5)	1.490(1)	1.439(4)	1.448(8)
C ₅ -C ₆	1.426(6)	1.460(5)	1.426(5)	1.472(2)	1.436(4)	1.422(6)
C ₆ -C ₁	1.373(7)	1.366(5)	1.417(6)	1.474(1)	1.436(4)	1.422(6)
C-C _{ave}	1.41(4)	1.44(5)	1.426(8)	1.479(9)	1.442(6)	1.43(1)
Ti ₁ ...Ti ₂	-	-	3.588(2)	3.4762(3)	3.6419(6)	3.654(3)
arene dihedral angle	19.8(2)	29.6(3)	9.2(3)	- ^a	20.0(2)	16.1(11)

^aDihedral angle is negligible

Computational Methods

All geometry optimizations and frequency calculations were performed with the Gaussian 16 package (Rev. C.016).⁹ Structures were optimized using the M06 functional¹⁰ and def2- family of basis sets,¹¹⁻¹² generally starting with def2sv(p) and reoptimizing at the def2svp level. The ultrafine grid setting was used for all calculations to avoid integration errors, as is suggested with M06 functionals.¹³⁻¹⁴ Calculations on compounds with unpaired electrons were ran using unrestricted DFT, with a representative orbital belonging to one electron shown (α in most cases). Frequency calculations were performed on the optimized geometries at the same level of theory to obtain free energies and verify the structure as a minimum with no imaginary frequencies. To mitigate fictitious contributions by small frequencies, thermal energies were calculated at 298.15 K and 1 atm using a frequency correction calculation that scales any frequencies lower than 50 cm⁻¹ to 50 cm⁻¹.¹⁵ Figures of computational structures have hydrogens omitted for clarity and MOs rendered at an iso value of 0.02.

Computational Investigation

The goal of our computational investigation was to obtain DFT-optimized structures of both the titanium toluene adduct and side on N₂ adduct [5 and 6]. While not as convincing as experimental results, this would help us compare structural data and see if the calculated structures optimized to our expected structures and were local minima on their respective potential energy surfaces. Additionally, this would allow a qualitative understanding of bonding in 5 and 6. Optimization of 6 both as **6-Li** and **6-K** from X-ray coordinates using the M06 functional starting at the def2sv(p) level before reoptimizing with def2svp resulted in the same overall structure from X-ray coordinates (Figure S5, top). Attempts to optimize the side on N₂ adduct 5 either as a doublet or as a quartet resulted in vastly different structures (Figure S5, bottom). Initial optimizations from X-ray coordinates were unsuccessful with the standard Berny algorithm, and required the keyword scf=xqc as the SCF was not able to converge otherwise.

The doublet structure optimizes to give a bridging N₂ between the two Ti atoms and an equivalent of N₂ extruded, with the closest Ti-N contact at over 3 angstroms. The quartet structure optimizes

to give a $\mu_2\text{-}\eta^2\text{:}\eta^1$ coordinated dinitrogen ($\text{N-N} = 1.237 \text{ \AA}$). The other N_2 could be described as a $\mu_2\text{-}\eta^1\text{:}\eta^1$ coordinated dinitrogen ($\text{N-N} = 1.19 \text{ \AA}$) with one elongated Ti-N interaction at 2.14 \AA . Both of these results and the fact that quadratic convergence is necessary when starting from the previously reported coordinates provides further evidence that **5** is unlikely to exist.

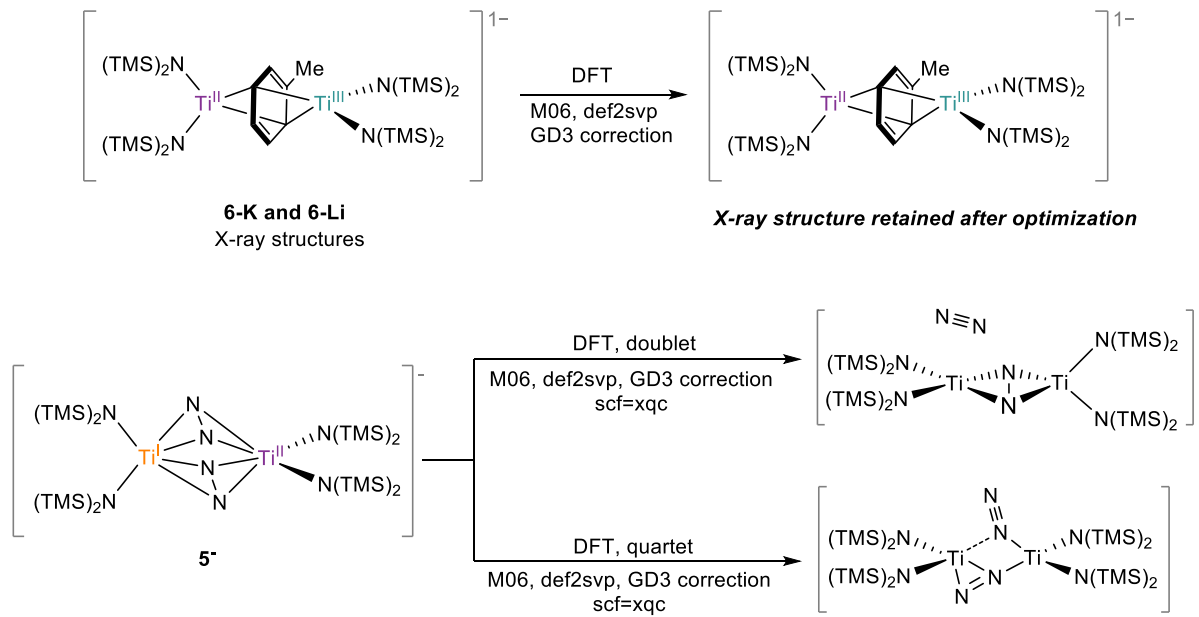


Figure S7. Summary of DFT analyses of **6-Li**, **6-K**, and **5-**.

Qualitative analysis of the frontier orbitals of **6-K** and **6-Li** demonstrates that, as expected, the bonding is extremely similar. The LUMO and SOMO β (unoccupied) are cation centered, either on the K^+ -capping arene, or TMEDAs wrapped around Li^+ . The SOMO α (occupied) for both compounds involves one Ti-arene σ -interaction and δ -bonding between the other Ti and arene. The HOMOs involve almost entirely Ti-arene δ -bonding, as do the HOMO-1s. Below HOMO-1, the MOs are primarily Ti-amide bonding or ligand centered.

Frontier Orbitals of 6-Li

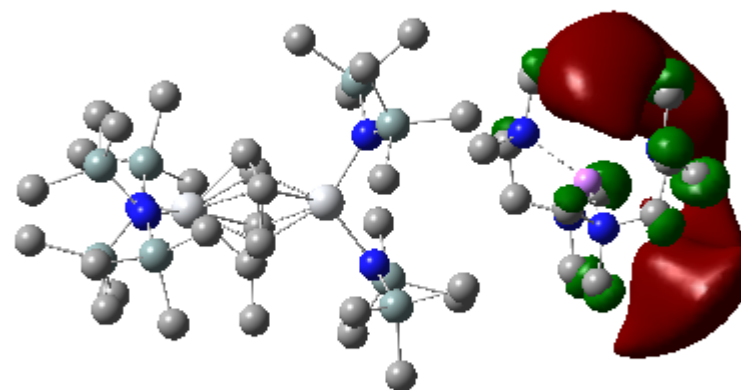
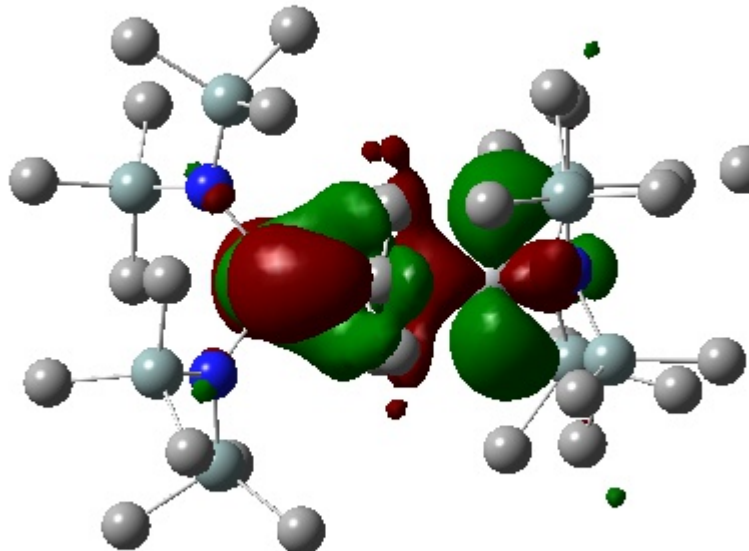


Figure S8. SOMO β (unoccupied) centered on ligands of Li^+ .



Figures S9. SOMO α (occupied) showing delta bonding between one Ti atom and arene, and sigma bonding between other Ti atom and arene. $\text{Li}(\text{TMEDA})_2^+$ omitted.

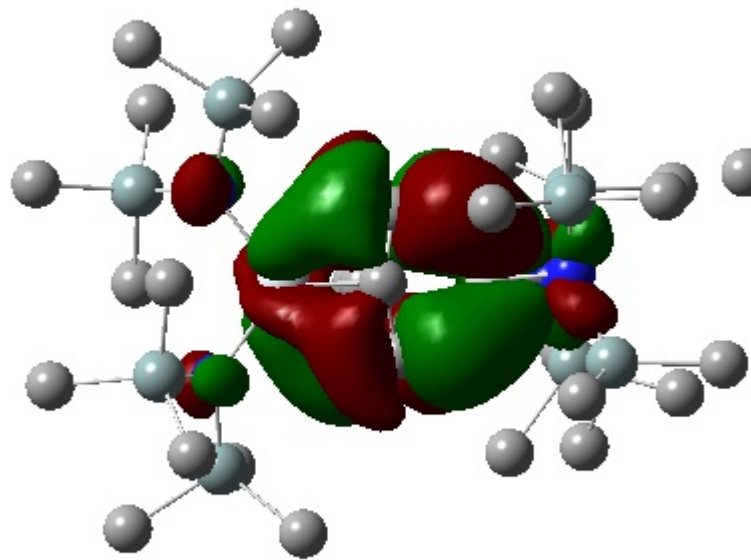


Figure S10. HOMO showing delta bonding between both Ti atoms and arene.
 $\text{Li}(\text{TMEDA})_2^+$ omitted.

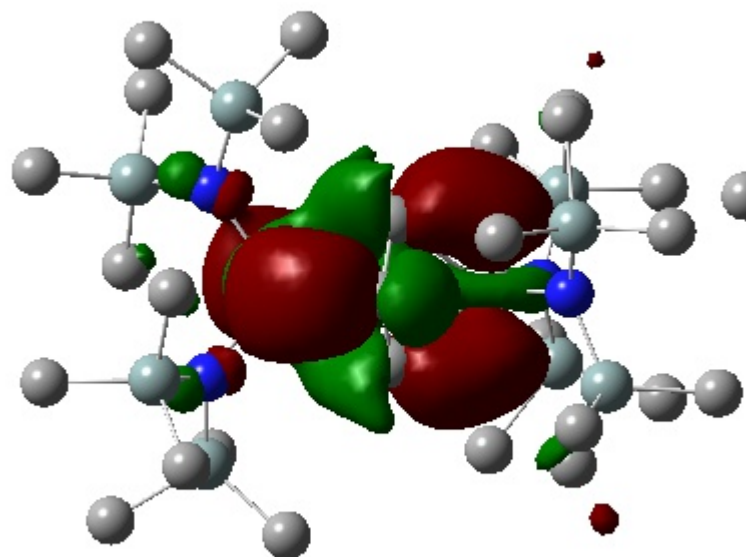


Figure S11. HOMO-1 showing delta bonding between both Ti atoms and arene.
 $\text{Li}(\text{TMEDA})_2^+$ omitted

Frontier Orbitals of 6-K

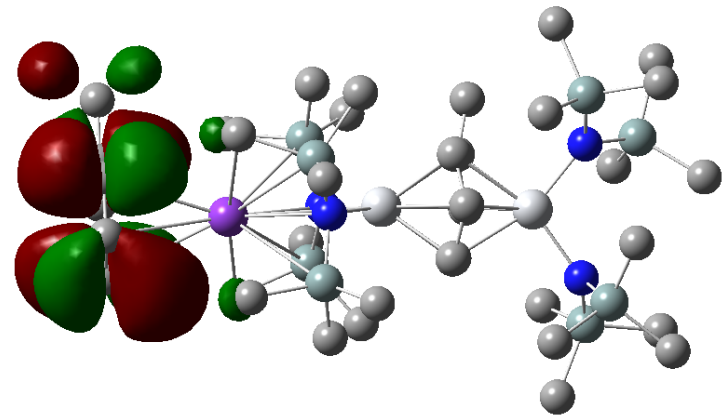


Figure S12. LUMO centered on arene interaction with K⁺.

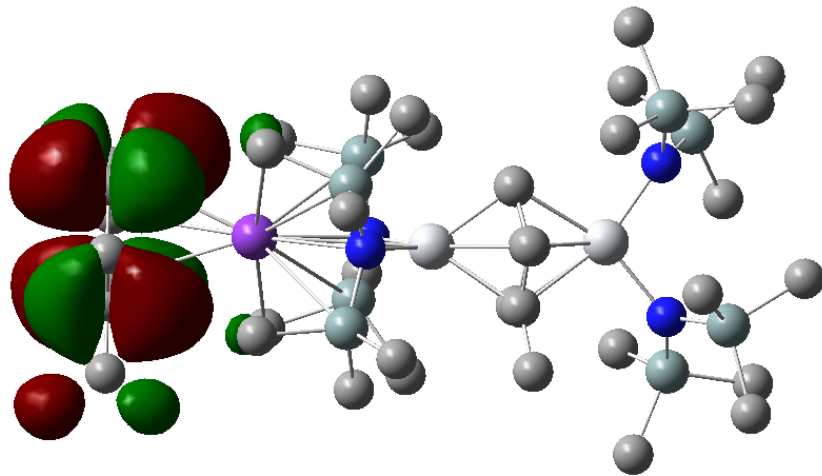


Figure S13. SOMO β (unoccupied) centered on the arene interaction with K⁺.

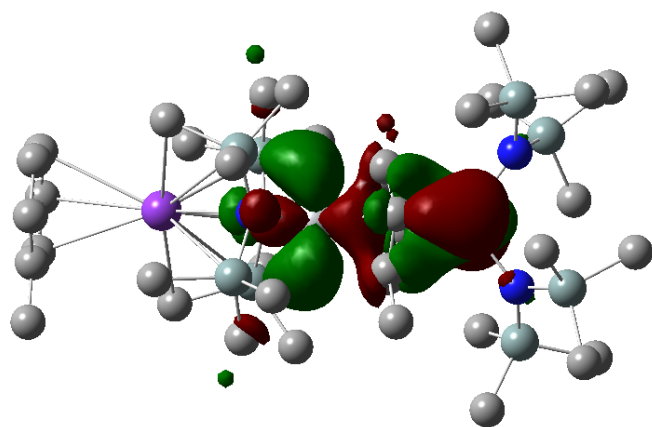


Figure S14. SOMO α (occupied) showing delta bonding between one Ti atom and arene, and sigma bonding between other Ti atom and arene.

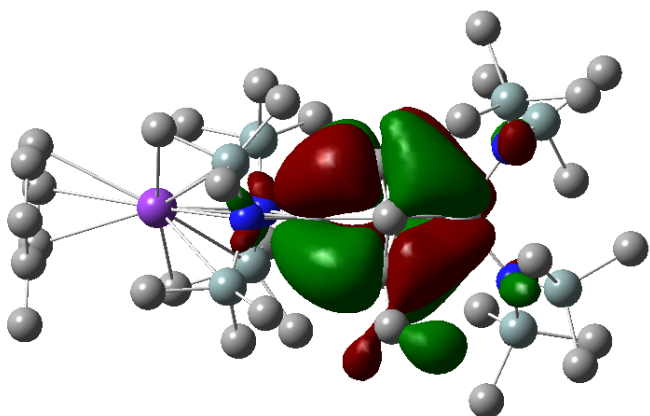


Figure S15. HOMO showing delta bonding between both Ti atoms and arene.

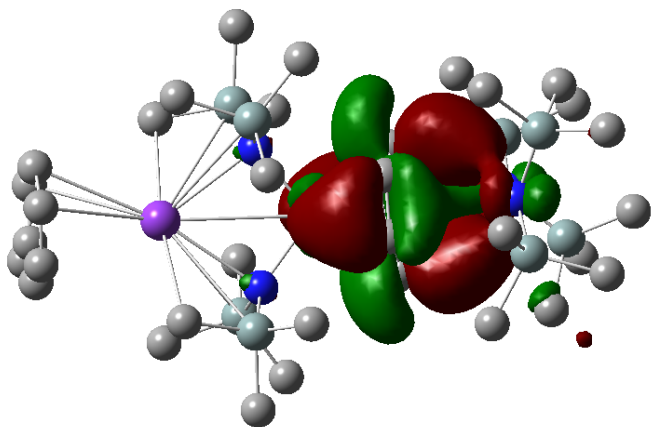


Figure S16. HOMO-1 showing delta bonding between both Ti atoms and arene.

5⁻ quartet

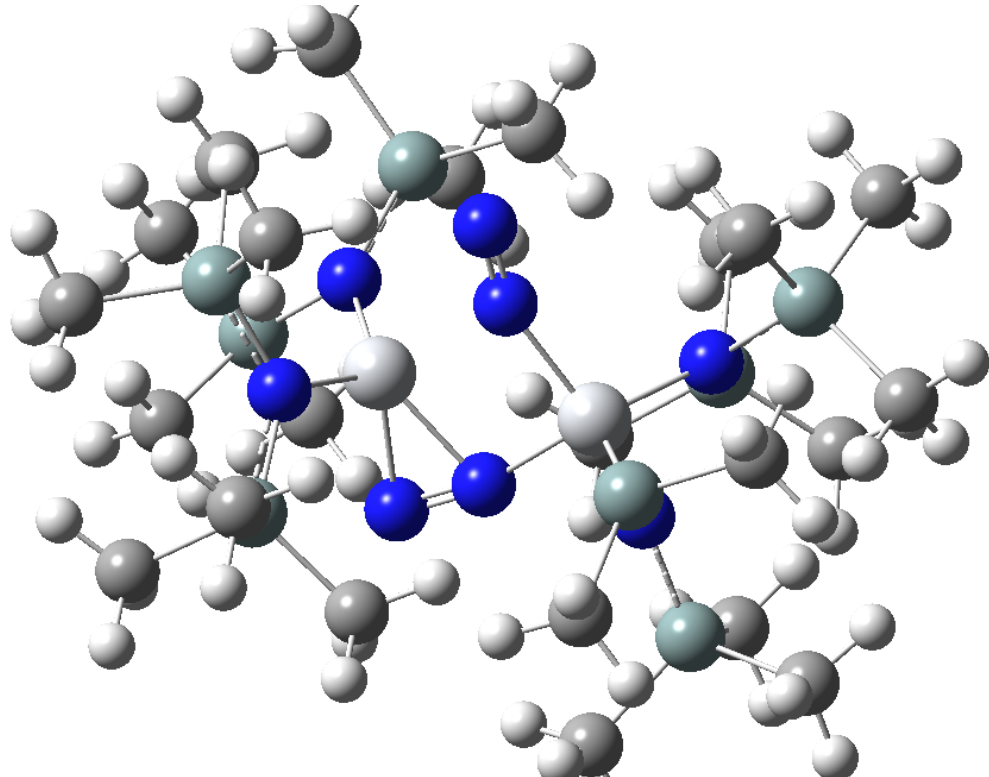


Figure S17. The calculated structure of 5⁻ as a quartet from crystallographic coordinates optimizes to yield a coordinated end-on dinitrogen and $\mu_2\text{-}\eta^2\text{:}\eta^1$ coordinated dinitrogen.

5⁻ doublet

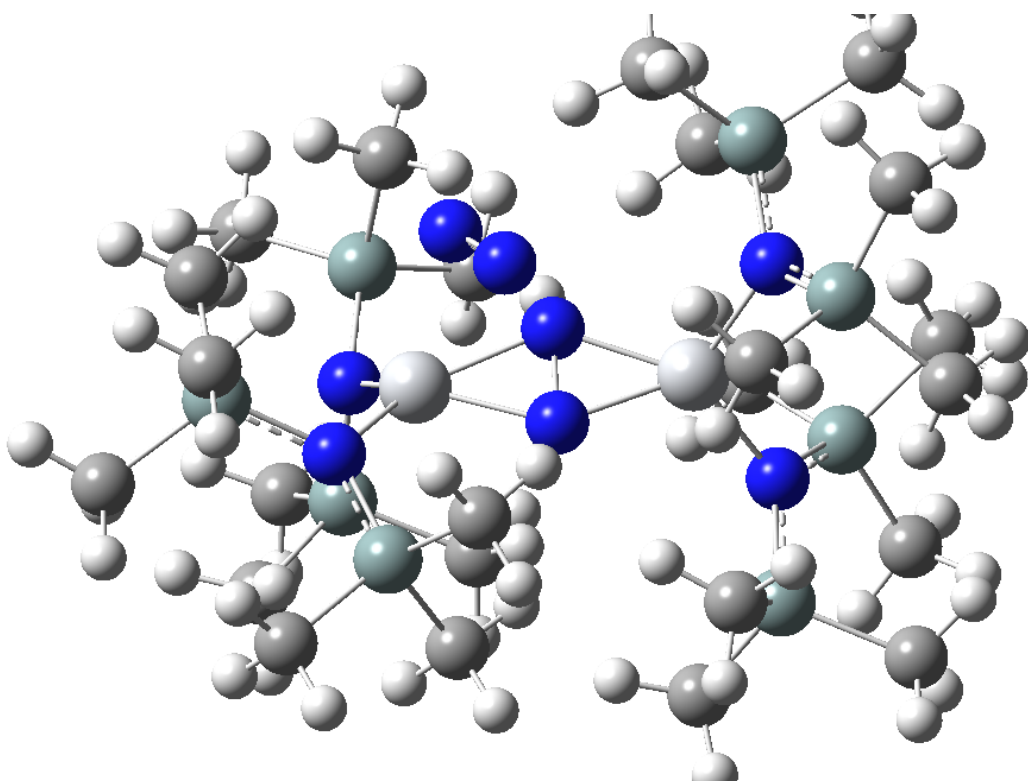


Figure S18. The calculated structure of **5⁻** as a doublet from crystallographic coordinates optimizes to yield a dissociated dinitrogen (3.12 Å to closest Ti) and bridging nitrides.

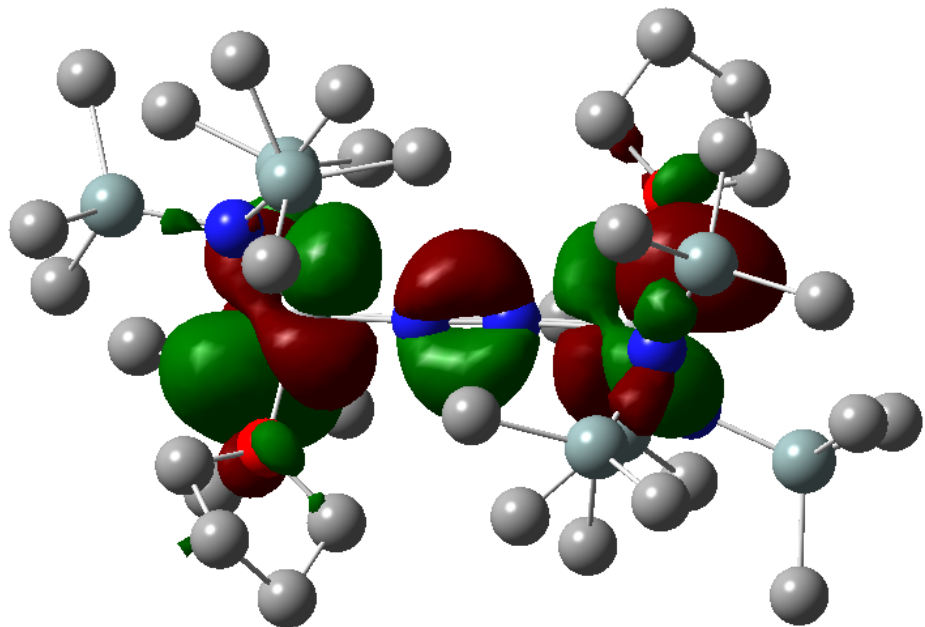


Figure S19. LUMO of **10** depicting N–N pi bonding and Ti–N pi anti-bonding.

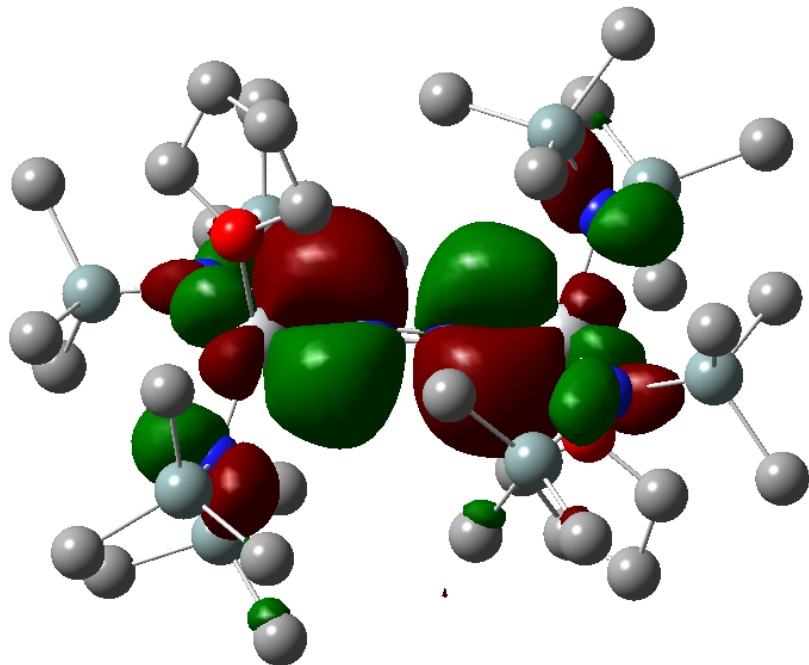


Figure S20. HOMO of **10** depicting Ti–N pi bonding.

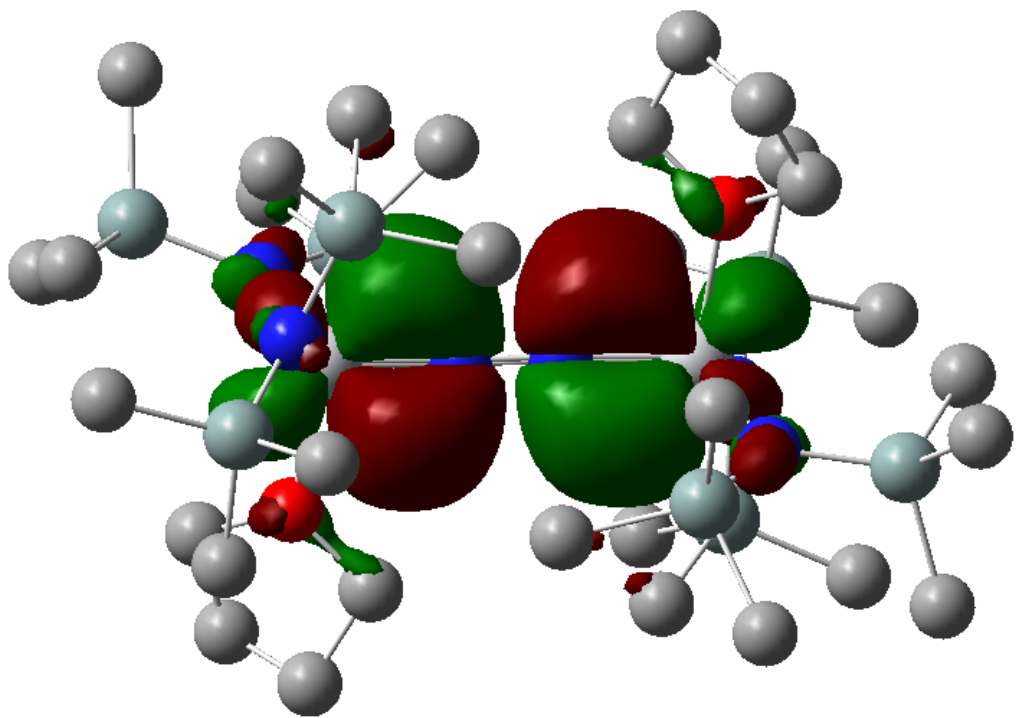


Figure S21. HOMO-1 of **10** depicting Ti–N pi bonding (orthogonal to HOMO).

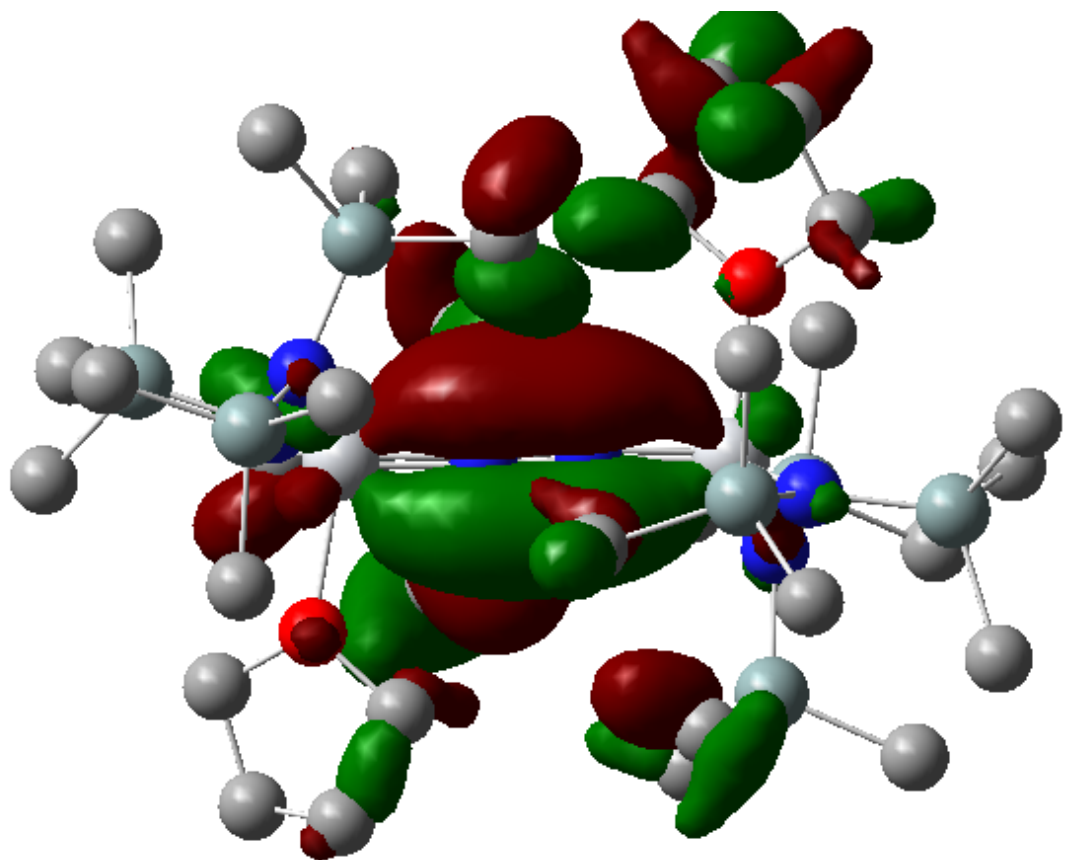


Figure S22. HOMO-33 of **10** depicting continuous Ti–N–N–Ti pi bonding.

UV-VIS DATA

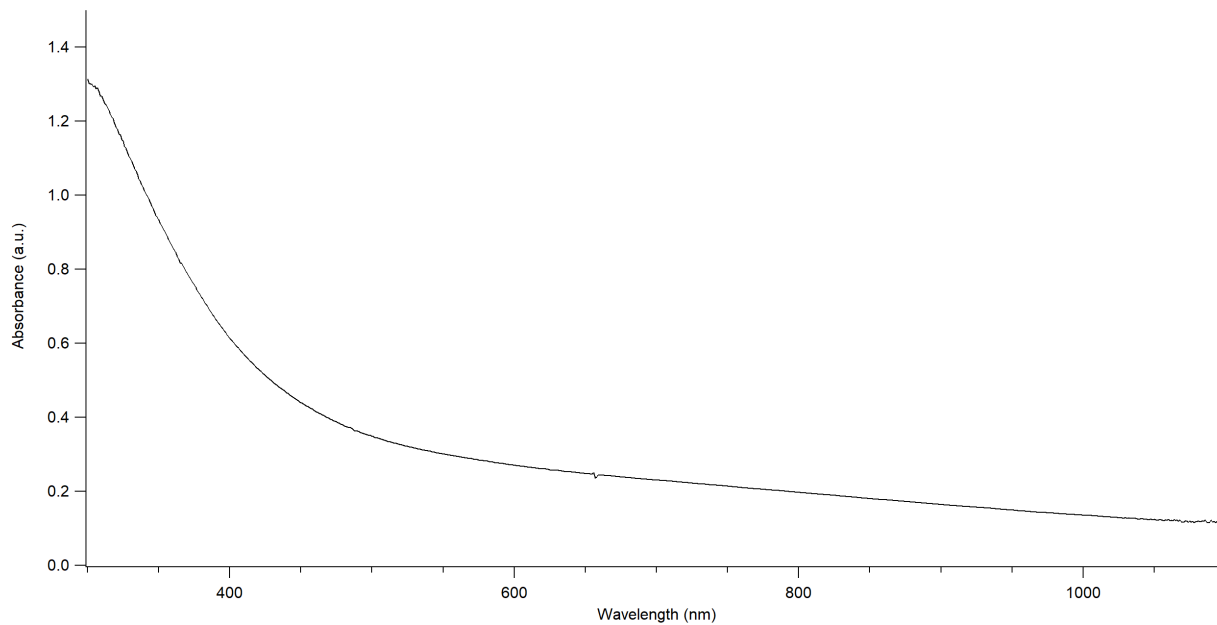


Figure S23. UV-vis spectrum of **6-K** in toluene.

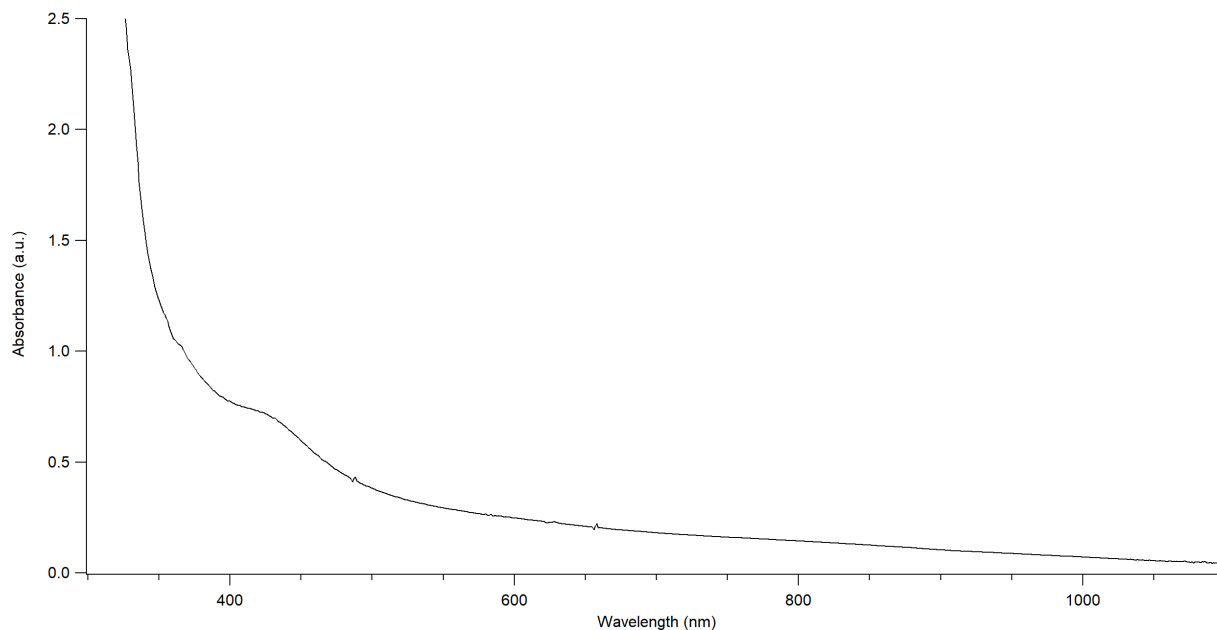


Figure S24. UV-vis spectrum of **6-Li** in 10:1 toluene:TMEDA.

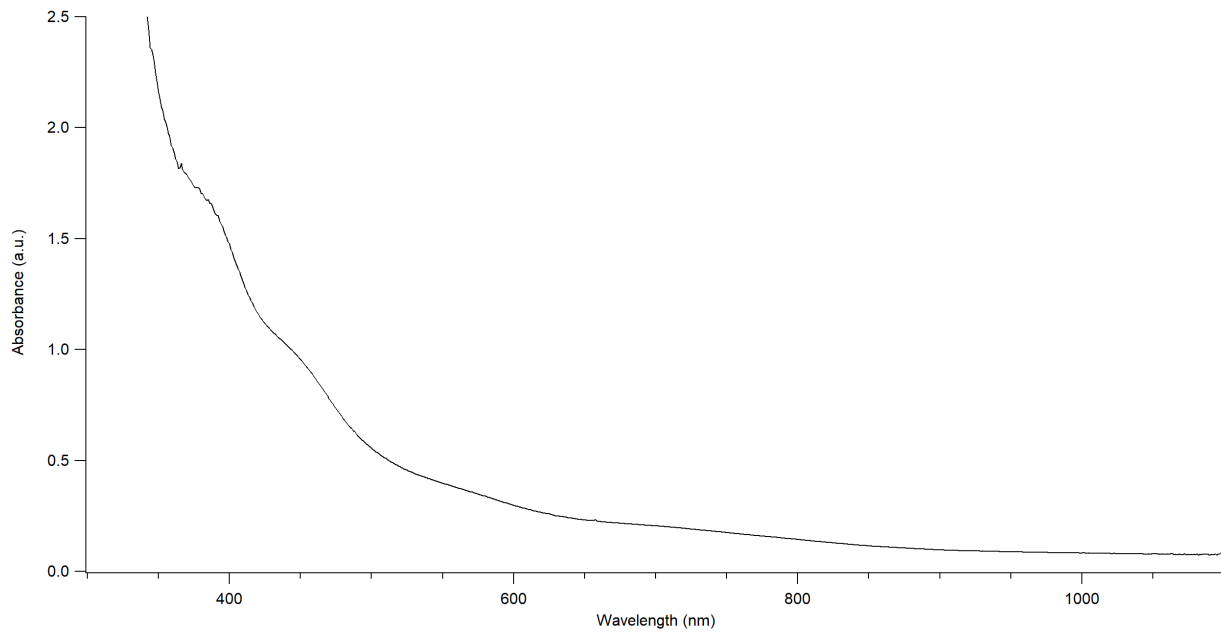


Figure S25. UV-vis spectrum of **10** in pentane.

RAMAN DATA

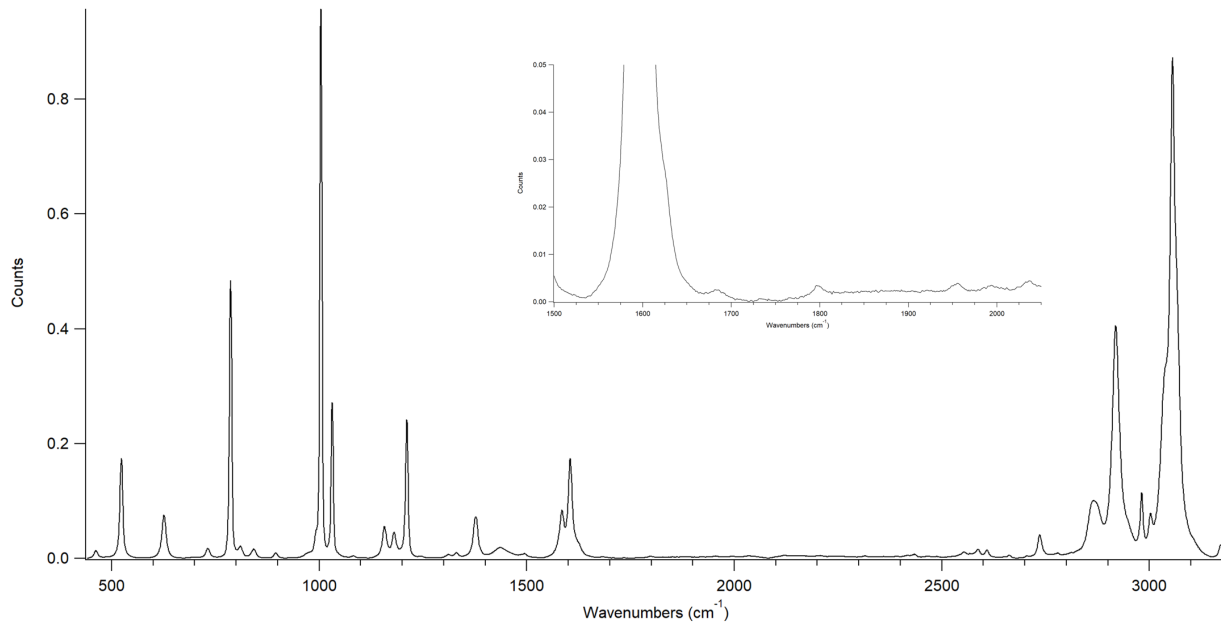


Figure S26. Raman of **6-K** in toluene using a 457 nm laser and expanded region (inset). Note: solvent background not subtracted.

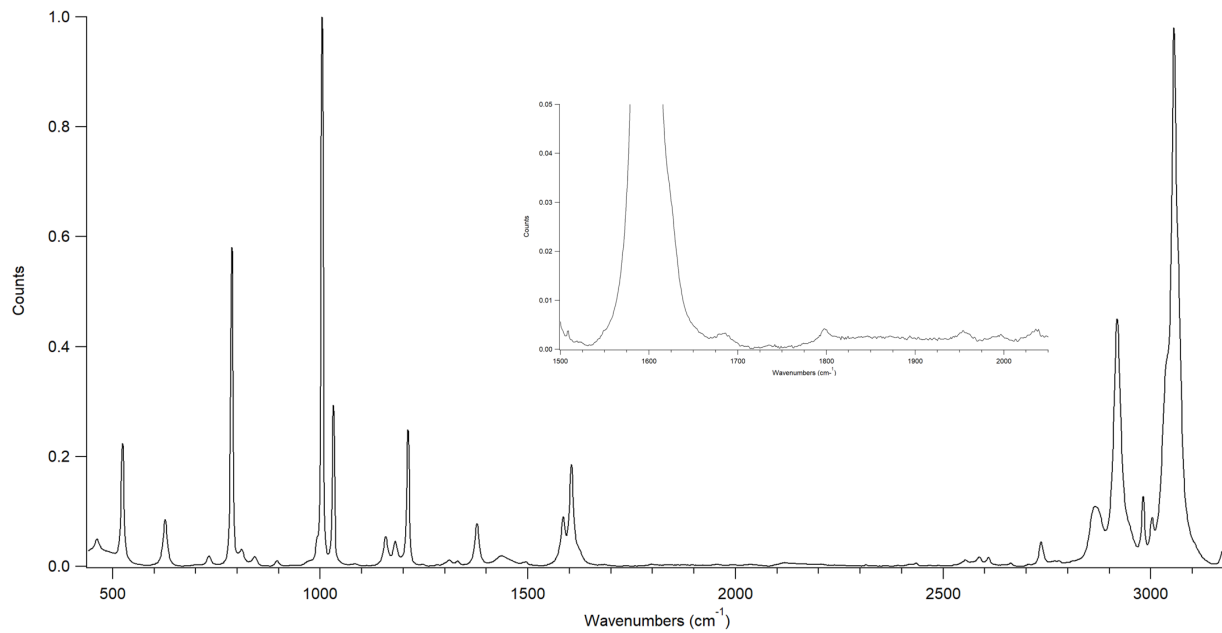


Figure S27. Raman of **6-Li** in 10:1 toluene:TMEDA using a 457 nm laser and expanded region (inset). Note: solvent background not subtracted.

Table S16. Comparison of select $\nu_{\text{N-N}}$ frequencies (cm^{-1}) and N–N bond distances (\AA) of bimetallic Ti complexes containing a $\mu_2\text{-N}_2$.

Compound	$\nu_{\text{N-N}}$ (cm^{-1})	N–N (\AA)	Side-on or End-on N_2	Reference
$[(\text{Tren}^{\text{TMS}})\text{Ti}]_2(\mu\text{-}\eta^1\text{:}\eta^1\text{-}\text{N}_2)$	1701	1.121(6)	end-on	16
$[(\eta^5\text{-C}_5\text{Me}_4\text{Et})_2\text{Ti}(\text{N}_2)](\eta^1\text{:}\eta^1\text{-}\text{N}_2)$	1719	1.150(2)	end-on	17
$[(\eta^5\text{-C}_5\text{H}_3\text{-1-}\text{iPr-3-Me})_2\text{Ti}]_2(\eta^2\text{:}\eta^2\text{-}\text{N}_2)$	1742	1.226(5)	side-on	18
$[(\eta^5\text{-C}_5\text{H}_3\text{-1,3-}\text{iPr}_2)_2\text{Ti}]_2(\eta^2\text{:}\eta^2\text{-}\text{N}_2)$	1747	1.216(5)	side-on	18
$[(\eta^5\text{-C}_5\text{Me}_5)(\eta^6\text{-C}_5\text{H}_4\text{C}(\text{C}_6\text{H}_4\text{-4-Me})_2)\text{Ti}]_2(\eta^1\text{:}\eta^1\text{-}\text{N}_2)$	1749	1.160(3)	end-on	19
Free N_2	2330	1.098(1)	-	-

Routing keywords and energies: See XYZ file for coordinates

6-Li

```
opt=(calcfc,maxcyc=512) freq=noraman def2svp empiricaldispersion=gd3
integral=grid=ultrafinegrid m06 scf=maxcyc=512 temperature=298.15
```

Energies

The electronic energy (Hartrees):	-6162.80362
The Corrected Thermal Enthalpy (Hartrees):	-6161.220173
The Corrected Thermal Free Energy (Hartrees):	-6161.441666

6-K

```
opt=(calcfc,maxcyc=512) freq=noraman def2svp empiricaldispersion=gd3
integral=grid=ultrafinegrid m06 scf=maxcyc=512 temperature=298.15
```

Energies

The electronic energy (Hartrees):	-6331.779642
The Corrected Thermal Enthalpy (Hartrees):	-6330.530146
The Corrected Thermal Free Energy (Hartrees):	-6330.728273

5- doublet (initial coordinates from crystal structure)

```
opt=(calcfc,maxcyc=512) freq=noraman def2svp empiricaldispersion=gd3
integral=grid=ultrafinegrid m06 temperature=298.15 scf=xqc
```

Energies

The electronic energy (Hartrees): -5408.410285
The Corrected Thermal Enthalpy (Hartrees): -5407.414847
The Corrected Thermal Free Energy (Hartrees): -5407.596073

5· quartet (initial coordinates from crystal structure)

opt=(calcfc,maxcyc=512) freq=noraman def2svp empiricaldispersion=gd3
integral=grid=ultrafinegrid m06 temperature=298.15 scf=xqc

Energies

The electronic energy (Hartrees): -5408.410285
The Corrected Thermal Enthalpy (Hartrees): -5407.414847
The Corrected Thermal Free Energy (Hartrees): -5407.596073

10 from crystal structure

opt=(calcfc,maxcyc=512) freq=noraman def2svp empiricaldispersion=gd3
integral=grid=ultrafinegrid m06 temperature=298.15

Energies

The electronic energy (Hartrees): -5763.302627
The Corrected Thermal Enthalpy (Hartrees): -5762.066345
The Corrected Thermal Free Energy (Hartrees): -5762.259627

REFERENCES

1. M. T. Manuel Aristarán and Jeremy B. Merrill *Tabula*, 2018 <https://tabula.technology/>.
2. O. V. Dolomanov, L. J. Bourhis, R. J. Gildea, J. A. K. Howard and H. Puschmann. "OLEX2: a complete structure solution, refinement and analysis program." *Journal of Applied Crystallography* 2009, **42**, 339-341.
3. G. Sheldrick. "A short history of SHELX." *Acta Crystallographica Section A* 2008, **64**, 112-122.
4. A. Spek. "Single-crystal structure validation with the program PLATON." *Journal of Applied Crystallography* 2003, **36**, 7-13.
5. J. R. Hagadorn and J. Arnold. Tethered Bis-Amidinates as Supporting Ligands: A Concerted Elimination/ σ - π Rearrangement Reaction Forming an Unusual Titanium Arene Complex *Angew. Chem. Int. Ed.* 1998, **37**, 1729-1731.
6. O. V. Ozerov, B. O. Patrick, and F. T. Ladipo. Highly Regioselective [2 + 2 + 2] Cycloaddition of Terminal Alkynes Catalyzed by η^6 -Arene Complexes of Titanium Supported by Dimethylsilyl-Bridged p-tert-Butyl Calix[4]arene Ligand *J. Am. Chem. Soc.* 2000, **122**, 6423-6431.
7. R. Gyepes, J. Pinkas, I. Císařová, J. Kubišta, M. Horáček, and K. Mach. Synthesis, molecular and electronic structure of a stacked half-sandwich dititanium complex incorporating a cyclic π -faced bridging ligand *RSC Adv.* 2016, **6**, 94149-94159.
8. G. B. Nikiforov, P. Crewdson, S. Gambarotta, I. Korobkov, and P. H. M. Budzelaar. Reduction of Titanium Supported by a σ -/ π -Bonded Tripyrrole Ligand: Ligand C-N Bond Cleavage and Coordination of Olefin and Arene with an Inverse Sandwich Structure *Organometallics* 2007, **26**, 48-55.
9. M. J. Frisch, G. W. Trucks, H. B. Schlegel, G. E. Scuseria, M. A. Robb, J. R. Cheeseman, G. Scalmani, V. Barone, G. A. Petersson, H. Nakatsuji, X. Li, M. Caricato, A. V. Marenich, J. Bloino, B. G. Janesko, R. Gomperts, B. Mennucci, H. P. Hratchian, J. V. Ortiz, A. F. Izmaylov, J. L. Sonnenberg, Williams, F. Ding, F. Lipparini, F. Egidi, J. Goings, B. Peng, A. Petrone, T.

Henderson, D. Ranasinghe, V. G. Zakrzewski, J. Gao, N. Rega, G. Zheng, W. Liang, M. Hada, M. Ehara, K. Toyota, R. Fukuda, J. Hasegawa, M. Ishida, T. Nakajima, Y. Honda, O. Kitao, H. Nakai, T. Vreven, K. Throssell, J. A. Montgomery Jr., J. E. Peralta, F. Ogliaro, M. J. Bearpark, J. J. Heyd, E. N. Brothers, K. N. Kudin, V. N. Staroverov, T. A. Keith, R. Kobayashi, J. Normand, K. Raghavachari, A. P. Rendell, J. C. Burant, S. S. Iyengar, J. Tomasi, M. Cossi, J. M. Millam, M. Klene, C. Adamo, R. Cammi, J. W. Ochterski, R. L. Martin, K. Morokuma, O. Farkas, J. B. Foresman, and D. J. Fox. Gaussian 16 Rev. C.01, Wallingford, CT, 2016.

10. Y. Zhao and D. G. Truhlar, The M06 suite of density functionals for main group thermochemistry, thermochemical kinetics, noncovalent interactions, excited states, and transition elements: two new functionals and systematic testing of four M06-class functionals and 12 other functionals. *Theor. Chem. Acc.* 2008, **120**, 215-241.
11. F. Weigend and R. Ahlrichs. Balanced basis sets of split valence, triple zeta valence and quadruple zeta valence quality for H to Rn: Design and assessment of accuracy. *Phys. Chem. Chem. Phys.* 2005, **7**, 3297-3305.
12. F. Weigend. Accurate Coulomb-fitting basis sets for H to Rn. *Phys. Chem. Chem. Phys.* 2006, **8**, 1057-1065.
13. S. E. Wheeler and K. N. Houk. Integration Grid Errors for Meta-GGA-Predicted Reaction Energies: Origin of Grid Errors for the M06 Suite of Functionals. *J. Chem. Theor. Comp.* 2010, **6**, 395-404.
14. N. Mardirossian and M. Head-Gordon. How Accurate Are the Minnesota Density Functionals for Noncovalent Interactions, Isomerization Energies, Thermochemistry, and Barrier Heights Involving Molecules Composed of Main-Group Elements? *J. Chem. Theor. Comp.* 2016, **12**, 4303-4325.
15. R. F. Ribeiro, A. V. Marenich, C. J. Cramer, and D. G. Truhlar. Use of Solution-Phase Vibrational Frequencies in Continuum Models for the Free Energy of Solvation. *J. Phys. Chem B* 2011, **115**, 14556-14562.

16. L. R. Doyle, A. J. Wooles, L. C. Jenkins, F. Tuna, E. J. L. McInnes, and S. T. Liddle. Catalytic Dinitrogen Reduction to Ammonia at a Triamidoamine-Titanium Complex. *Angew. Chem. Int. Ed.* 2018, **57**, 6314-6318.
17. T. E. Hanna, E. Lobkovsky, and P. J. Chirik. Dinitrogen Complexes of Bis(cyclopentadienyl) Titanium Derivatives: Structural Diversity Arising from Substituent Manipulation. *Organometallics*, 2009, **28**, 4079-4088.
18. S. P. Semproni, C. Milsmann, and P. J. Chirik. Side-on Dinitrogen Complexes of Titanocenes with Disubstituted Cyclopentadienyl Ligands: Synthesis, Structure, and Spectroscopic Characterization. *Organometallics*, 2012, **31**, 3672-3682.
19. F. Studt, N. Lehnert, B. E. Wiesler, A. Scherer, R. Beckhaus, F. Tuczek. *Eur. J. Inorg. Chem.* 2006, 291-297.